IECON
DOCUMENTOS
DE INVESTIGACIÓN
ESTUDIANTIL

DIE 01/26
Marzo, 2026
ISSN: 2301-1963

Carry Trade and Exchange Rate Dynamics: The Case of Uruguay

Federico Riella

FCEA FACULTAD DE CIENCIAS ECONÓMICAS Y DE ADMINISTRACIÓN
IECON INSTITUTO DE ECONOMÍA
UNIVERSIDAD DE LA REPÚBLICA URUGUAY

Agradezco especialmente a mi tutor, Fernando Lorenzo, por su incansable disposición a contribuir al desarrollo de esta tesis. También agradezco a todo el equipo de CINVE y, en particular, a Rafael Mosteiro por sus valiosos comentarios. Cualquier error u omisión, así como todas las opiniones aquí expresadas, son de exclusiva responsabilidad del autor. Agradezco también a la Facultad de Ciencias Económicas y de Administración y a la Comisión Académica de Posgrados por el apoyo brindado para la realización de esta tesis. Finalmente, agradezco a mi familia y amigos, pilar fundamental de mis logros en general y de este en particular.

Forma de citación sugerida para este documento: Riella, F. (2026). "Carry Trade and Exchange Rate Dynamics: The Case of Uruguay". Serie Documentos de Investigación Estudiantil, DIE 01/26. Instituto de Economía, Facultad de Ciencias Económicas y Administración, Universidad de la República, Uruguay.

Suggested citation format for this document: Riella, F. (2026). "Carry Trade and Exchange Rate Dynamics: The Case of Uruguay". Serie Documentos de Investigación Estudiantil, DIE 01/26. Instituto de Economía, Facultad de Ciencias Económicas y Administración, Universidad de la República, Uruguay.

Carry Trade and Exchange Rate Dynamics: The Case of Uruguay

Federico Riella

Master's Thesis submitted to the Master's Program in Economics at Facultad de Ciencias Económicas y de Administración, Universidad de la República, as part of the requirements for the degree of Master in Economics.

Resumen

La estrategia de carry trade consiste en invertir en activos denominados en una moneda con una tasa de interés relativamente alta, financiando dicha inversión con deuda en una moneda con una tasa de interés más baja. Los cambios en la demanda de moneda doméstica asociados a operaciones de carry trade generan períodos de apreciaciones graduales seguidos de depreciaciones súbitas. Este estudio presenta evidencia de que estas dinámicas tienen lugar para el tipo de cambio USD/UYU durante el período más reciente en el que la tasa de interés se ha utilizado como instrumento de política monetaria. Posteriormente, mediante un enfoque innovador para estimar el carry-to-risk ratio, utilizado como proxy de los incentivos al carry trade, muestro que, en este período, existe una relación positiva entre la demanda por instrumentos denominados en pesos y los incentivos para realizar carry trade. Esta evidencia respalda la idea de que las operaciones de carry trade ayudan a explicar la relación negativa entre el diferencial de tasas de interés y tanto la media como la varianza del tipo de cambio. Estos hallazgos son relevantes dada la posibilidad de depreciaciones súbitas que tales dinámicas pueden desencadenar las cuales el banco central podría mitigar mediante una intervención oportuna.

Palabras clave: Carry trade; Carry-to-risk ratio; dinámica del tipo de cambio; diferencial de tasas de interés.

JEL Classification: F31, F32, G15, C32, E43, E44.

—

*Facultad de Ciéncias Económicas y de Administración, Universidad de la República, Uruguay, riellafederico@gmail.com

Abstract

The currency carry trade strategy is based on investing in assets denominated in a currency with a relatively high interest rate, financed with debt in a currency with a lower interest rate. Changes in demand for domestic currency associated with carry trade operations generate periods of gradual appreciations followed by sudden depreciations. This study shows evidence supporting that these dynamics take place for the USD/UYU exchange rate during the most recent period in which the interest rate has been used as the monetary policy instrument. Subsequently, through an innovative approach to estimating the carry-to-risk ratio, used as a proxy for carry trade incentives, I show that there is a positive relationship in this period between the demand for peso-denominated instruments and the incentives for carry trade. This evidence supports the view that carry trade operations help explain the negative relationship between the interest rate differential and both the mean and the variance of the exchange rate. These findings are relevant given the possibility of sudden depreciations that such dynamics can trigger, which the central bank could mitigate through timely intervention.

Keywords: Carry trade; Carry-to-risk ratio; Exchange rate dynamics; Interest rate differential.

JEL Classification: F31, F32, G15, C32, E43, E44.

Contents

1 Introduction

Dramatic exchange rate movements can occur in the absence of contemporaneous news about fundamentals, as documented empirically by Brunnermeier et al. (2009) and theoretically rationalized through the funding liquidity channel proposed by Brunnermeier and Pedersen (2008). In particular, abrupt unwinding of leveraged carry positions near funding constraints can generate large exchange rate movements that appear disconnected from macroeconomic announcements.

Currency carry trade, in its canonical form, consists of borrowing in a low interest rate funding currency and investing in a higher interest rate target currency.[1] In this way, investors profit from the interest rate differential as long as the exchange rate does not move adversely. In foreign exchange markets, speculators (typically leveraged investors and hedge funds) act as key liquidity providers, taking long and short positions across currencies in response to expected returns. Such trading operations require capital. Intermediaries that fund speculators' trades post margins or "haircuts" that tighten when volatility rises or risk appetite falls. While speculators have abundant capital, market liquidity is high and prices (in our case exchange rates) track fundamentals more closely. When funding constraints tighten, leveraged investors are forced to cut their positions to meet higher margin requirements. This deleveraging reduces market liquidity, making prices increasingly driven by liquidity conditions rather than fundamentals, which amplifies price movements only weakly related to fundamentals (Brunnermeier and Pedersen, 2008).

During the recent period in which the interest rate has served as the central monetary policy instrument (September 2020 onward), Uruguay has maintained a higher interest rate than the United States.[2] In a frictionless, risk neutral with perfect capital mobility setting, a positive interest rate differential should attract capital, induce an immediate appreciation, and be followed by a depreciation so that uncovered interest parity (UIP) holds on average. With liquidity constraints, however, capital arrives slowly; the exchange rate may appreciate only gradually. As frictions allow for profits, carry positions are maintained, and the investment currency can fail to depreciate at the UIP rate, allowing mispricing to persist. As rationalized by Abreu and Brunnermeier (2002), coordination frictions (synchronization risk) delay correction even for rational arbitrageurs, which helps explain why positions can build up and then unwind abruptly. These dynamics are consistent with the crash risk view of carry returns in Brunnermeier et al. (2009).

[1] Throughout, "carry trade" refers exclusively to currency carry trade. Equity or fixed income carry strategies are outside the scope of this study.

[2] In this thesis, the term interest rate refers to the monetary policy reference rate. The underlying data is provided in the appendix.

Given the risk of sudden depreciations associated with carry trade positions, detecting whether these operations are taking place has important macrofinancial implications, particularly in small open economies such as Uruguay, where even small capital flows in the foreign exchange market can significantly affect monetary and financial stability. The general objective of this work is to assess whether carry trade operations could be shaping the behavior of the USD/UYU exchange rate. This would be achieved by answering the following question: do increases in carry trade incentives generate higher demand for peso-denominated Monetary Regulation Bills (LRMs)? To pursue the general objective, three specific objectives are delimited. The first objective is to characterize the exchange rate dynamics during the period, constructing a GARCH model that accurately captures these dynamics. This first step will allow me to test the hypothesis that a higher interest rate differential is associated with a lower mean and lower variance of the exchange rate. Subsequently, based on the conditional volatility produced by this model, an indicator of carry trade incentives is constructed. Finally, local projections of LRMs demand on this indicator are estimated to assess whether increases in carry trade incentives generate an impact on the demand for domestic currency. By confirming this hypothesis, I support that exchange rate dynamics identified in the first step are driven by carry trade activity.

The main results show that both the mean and volatility of the USD/UYU exchange rate are significantly influenced by the interest rate differential between Uruguay and the United States. A higher differential is associated with a lower expected depreciation and reduced conditional volatility, consistent with the theoretical prediction that tighter monetary policy attracts capital inflows and stabilizes the exchange rate. The estimated GARCH(1,1) model confirms this relationship, with a stationary but persistent volatility process. Using the conditional volatility provided by the model, the carry-to-risk ratio (CTR) is constructed as a forward-looking indicator of carry trade incentives. Increases in the CTR are found to generate a significant rise in demand for peso-denominated LRMs. These results support the hypothesis that carry trade operations are an important channel linking interest rate policy and exchange rate dynamics in Uruguay.

The rest of this work is organized as follows. Section 2 provides the Background, reviewing the relevant literature on carry trade, crash risk, and local projections. Section 3 develops the Theoretical Framework, linking UIP deviations to the carry trade mechanism and outlining the liquidity-spiral and coordination-failure dynamics that underlie sudden exchange rate adjustments. Section 4 presents the empirical Identification strategy, describes the data, and introduces the GARCH model used to estimate conditional volatility and construct the carry-to-risk ratio. Section 5 reports the main results from local projections, showing how increases in carry trade incentives affect LRMs demand across maturity buckets. Finally, Section 6 concludes by summarizing the key findings and briefly mentioning their policy implications for exchange rate stability and central bank intervention.

2 Background

This study uses the carry-to-risk ratio as a proxy for carry trade incentives, consistent with the idea that excess returns in foreign exchange markets are linked to compensation for crash risk and financial constraints. Brunnermeier et al. (2009) show that carry strategies load on downside (crash) risk and display negative skewness; unwind episodes cluster when funding conditions tighten. This connects to the liquidity spiral mechanism of Brunnermeier and Pedersen (2008), where market and funding liquidity are mutually reinforcing: tighter margins and reduced risk appetite amplify price moves and force deleveraging. These limits-to-arbitrage considerations echo the synchronization risk of Abreu and Brunnermeier (2002), where arbitrageurs delay correcting mispricing due to coordination frictions, allowing positions (including carry) to build up and unwind abruptly.

The idea that carry trade returns reflect compensation for risk rather than arbitrage profits helps rationalize why these strategies persist despite the apparent violations of UIP. Empirical evidence of UIP failures has emerged from two complementary approaches. Regression-based tests (time-series), originating in Fama (1984), highlight the forward premium puzzle: high-interest-rate currencies tend to appreciate rather than depreciate, yielding predictable excess returns contrary to UIP. This anomaly has inspired a large literature on time-varying currency risk premia, including Engel (1996) and Burnside et al. (2011), which explore the robustness and theoretical implications of the forward premium regression. In parallel, portfolio-based analyses (cross-section), initiated by Lustig and Verdelhan (2007), focus on carry trade returns. By sorting currencies into portfolios based on interest rate differentials, these studies show that borrowing in low-interest-rate currencies and lending in high-interest-rate ones generates systematically positive returns, with high Sharpe ratios and exposure to crash risk. These findings point to persistent cross-currency risk premia that standard arbitrage-based theory must explain.

Hassan and Mano (2014) provide a unifying framework that bridges the regression- and portfolio-based perspectives. They decompose UIP deviations into three orthogonal components: a cross-currency component capturing persistent differences across currencies (which drives the profitability of carry trades), a cross-time component linked to global cycles and dollar-specific trends (relevant for the forward premium puzzle), and a negligible interaction term. Crucially, they show that carry trade returns are mostly driven by the static, cross-currency component, while the forward premium puzzle is explained by the time-varying component. This decomposition provides a coherent mapping between trading strategies and regression anomalies, helping reconcile stylized facts from both empirical approaches.

Building on this insight, the present study applies the unified view of Hassan and Mano (2014) to a bilateral, spot-market setting like Uruguay's, where forward markets are thin. It focuses on the static component of UIP deviations and evaluates whether persistent interest rate differentials not offset by depreciation give rise to carry trade incentives. To operationalize this, I follow Curcuru et al. (2010) in constructing a forward-looking carry-to-risk ratio (CTR) that accounts for both the potential return and the conditional risk of the strategy. This approach has been extended to Latin American contexts by Díaz et al. (2013), who show for Chile that increases in the CTR coincide with reductions in nonresident forward positions at key dates (e.g. 2010 and 2012), highlighting that heightened incentives can coexist with episodes of position-unwinding when market risk rises. Complementing this, Carreño and Cox (2014) document that positive interest differentials are associated with positive conditional skewness and that spikes in global risk are accompanied by sharp reductions in nonresident NDF positions, linking carry dynamics to exchange-rate turbulence. For Colombia, Gamboa-Estrada (2016) finds that high CTR values—combined with volatility, CDS spreads, and oil prices—are associated with elevated currency crash-risk, further underscoring the non-linear and state-dependent nature of carry trade exposure. For Uruguay, Fernández et al. (2023) highlight the correlation between the USD/UYU decline and the bilateral interest rate differential but argue for a broader portfolio-adjustment channel. This study complements that view by explicitly modeling conditional volatility and isolating carry incentives through the CTR.

To trace the effect of carry incentives on local asset demand, we employ the local projections (LP) method of Jordà (2005), which offers robustness to model misspecification and flexibility across horizons. This method has become standard in macro-finance applications, including exchange rate and monetary policy studies (Plagborg-Møller and Wolf, 2021; Ramey, 2016). In our context, LPs allow us to estimate the dynamic response of LRM demand to shocks in the CTR across different maturities. For inference, we adopt the significance-band methodology proposed by Inoue et al. (2023), which improves joint hypothesis testing across horizons. This combination enables us to detect whether increases in carry incentives causally affect peso-denominated asset demand, thus validating the presence of carry trade activity and its relevance for exchange rate dynamics.

3 Theoretical Framework

This study argues that carry trade operations take place in Uruguay during the analysis period and that they affect the foreign exchange market. The fact that such operations are conducted implies that they are potentially profitable. Demonstrating that carry trades yield profits is not trivial, since these profits arise from a well-documented anomaly in the literature: the violation of UIP. I build on Hassan and Mano (2014) to provide a broad account of this anomaly and, once the problem is established, to identify which dimensions of the anomaly—and, subsequently, which trading strategies—are most relevant for the Uruguayan case. In particular, because forward markets are thin in Uruguay, I adapt the standard forward-based exposition to a spot-market framework, which is the appropriate setting for analyzing the Uruguayan exchange rate market. After deriving the reduced form of the anomaly for Uruguay, I show that it holds over the sample period.

The canonical Forward Premium Puzzle (Fama, 1984) regression is:

$$r_{x_{i,t+1}} \;=\; \alpha_i \;+\; \beta_i^{fpp}\,(f_{i,t}-s_{i,t}) \;+\; \varepsilon_{i,t+1}, \tag{1}$$

Here $r_{x_{i,t+1}} = f_{i,t} - s_{i,t+1}$ is the log excess return and $f_{i,t} - s_{i,t}$ the log forward premium. Substituting the expression for the excess return, which can be written as the forward–spot differential at time t minus the subsequent depreciation, we obtain:

$$r_{x_{i,t+1}} = (f_{i,t} - s_{i,t}) - \Delta s_{i,t+1}, \tag{2}$$

Using (2), the equation (1) can be rewritten in terms of the spot depreciation:

$$\Delta s_{i,t+1} \;=\; \alpha_i \;+\; \left(1-\beta_i^{fpp}\right)\left(f_{i,t}-s_{i,t}\right) \;+\; \varepsilon_{i,t+1}. \tag{3}$$

Empirically, the Fama regression often implies $\beta_i^{fpp} > 0$ (in many cases greater than one). In the spot-dependent form this corresponds to a coefficient $1 - \beta_i^{fpp} < 1$, which indicates that the interest differential is not fully offset by expected depreciation.

There are three dimensions of variation in (1): across currencies, between time and currency, and across time. Interestingly, as synthesized in Hassan and Mano (2014), each of these components aligns with a distinct anomaly in the UIP literature, and each one allows for profits through a different type of trade. The cross–currency component captures persistent differences across currencies and underlies the carry anomaly, which allows for the so-called static trade. This is the component that will be relevant for our analysis. The between–time–and–currency component allows for dynamic trade. It captures short–run deviations from currency–specific and global means and links the carry trade and the forward premium puzzle in a time–varying manner. Finally, the cross–time component (dollar trade) captures fluctuations in the global average premium around its long–run mean and is closely associated with the forward premium puzzle, as we will see. Considering this schema, two investment strategies can be written as:

$$\sum_{i,t}\left[r_{x_{i,t+1}}(fp_{i,t}-\bar{fp})\right]=\underbrace{\sum_{i,t}\left[r_{x_{i,t+1s}}(\bar{fp}_i-\bar{fp})\right]}_{\text{Static Trade}}+\underbrace{\sum_{i,t}\left[r_{x_{i,t+1}}(fp_{i,t}-\bar{fp}_i-(\bar{fp}_i-\bar{fp}))\right]}_{\text{Dynamic Trade}}, \tag{4}$$

which defines the *carry trade* as the sum of a static and a dynamic leg, and

$$\sum_{i,t}\left[r_{x_{i,t+1}}(fp_{i,t}-\bar{fp}_t)\right]=\underbrace{\sum_{i,t}\left[r_{x_{i,t+1}}(fp_{i,t}-\bar{fp}_i-(\bar{fp}_t-\bar{fp}))\right]}_{\text{Dynamic Trade}}+\underbrace{\sum_{i,t}\left[r_{x_{i,t+1}}(\bar{fp}_t-\bar{fp})\right]}_{\text{Dollar Trade}}, \tag{5}$$

which decomposes the *forward premium trade* into dynamic and dollar components. Here $fp_{i,t}=f_{i,t}-s_{i,t}$, $\bar{fp}_i$ is the currency specific time average, $\bar{fp}_t$ the cross-sectional mean at t, and $\bar{fp}$ the grand mean.

The first identity shows that weighting currency returns by each currency's forward premium relative to the global average is equivalent to combining two exposures: a static leg that captures persistent cross-currency differences (currencies with chronically higher premia versus those with lower premia) and a dynamic leg that captures transitory deviations of the current premium from both its own mean and the global mean, i.e., a timing component over short-run fluctuations. The second identity, which weights by the deviation from the period t global average, decomposes into a dynamic component analogous to the previous one and a dollar component that represents exposure to the common global factor—the level of the cross-sectional mean premium relative to its long-run mean. In sum, theoretically, the carry trade strategy is primarily supported by persistent cross-currency heterogeneity with a short-run timing adjustment, whereas the forward-premium trade combines the same dynamic element with an exposure to the global (dollar) cycle.

The specification of trading strategies developed in (4) and (5) outlines the map of all possible trading strategies that can be constructed based on the three anomalies underlying UIP (carry trade, dollar trade, and the forward premium puzzle). To evaluate relevant trading operations for the case of Uruguay, the first thing to mention is that the dynamic component is discarded, since Hassan and Mano (2014) find that it is not relevant to explain the profits of either the carry trade or the forward premium trade. On the other hand, for simplicity, I will conceive trading strategies as being always funded at the U.S. dollar and invested in Uruguayan peso. This means we are evaluating the dynamics associated with the static trade. The dollar trade is not explicitly analyzed under the assumption that, during the sample period, the forward premium of the Uruguayan peso remains high relative to its historical mean; therefore, empirically, in our bilateral setting it would result in the same operation as the static carry trade.

To empirically test the UIP deviation phenomenon that makes static trade profitable, I will express all previously derived anomalies in regression form and then develop a set of assumptions to test whether the anomaly holds in the Uruguayan case. My key step here is to move from Equation (1) to the decomposition of Hassan and Mano (2014) that relates regression facts to portfolio facts. In their work, the authors show that the portflio based decompsotion can be written as (6). Since when estimated with currency fixed effects, β_i^{fpp} reflects the elasticity of realized returns and does not correct for uncertainty about each currency's average premium, Hassan and Mano (2014) instead target expected returns and express the unconditional UIP violation as three orthogonal elasticities:

$$r_{x_{i,t+1}} = \gamma + \beta_{stat}\left(fp_i^e - fp^e\right) + \beta_{dyn}\left[(fp_{i,t} - fp_t) - (fp_i^e - fp^e)\right] + \beta_{dol}\left(fp_t - fp^e\right) + \varepsilon_{stat}^{i} + \varepsilon_{dyn}^{i,t+1} + \varepsilon_{dol}^{t+1}, \tag{6}$$

with expectations taken ex ante at t. The three component regressions are

$$r_{x_{i,t+1}} - r_{x_{t+1}} = \beta_{stat}\left(fp_i^e - fp^e\right) + \varepsilon_{stat}^{i,t+1}, \tag{7}$$

$$r_{x_{i,t+1}} - r_{x_{t+1}} - (r_{x_i} - r_x) = \beta_{dyn}\left[(fp_{i,t} - fp_t) - (fp_i^e - fp^e)\right] + \varepsilon_{dyn}^{i,t+1}, \tag{8}$$

$$r_{x_{t+1}} - r_x = \gamma + \beta_{dol}\left(fp_t - fp^e\right) + \varepsilon_{dol}^{t+1}, \tag{9}$$

where $r_{x_{t+1}}$ is the cross-sectional average excess return at $t+1$, r_x its long run mean, fp_t the cross sectional average forward premium at t, fp^e its long run expectation, and fp_i^e the long run expected premium of currency i. Intuitively, the regression form in equations (7)–(9) mirrors the same structure implied by the trading-strategy formulations in (4) and (5). Each regression coefficient $(\beta_{stat}, \beta_{dyn}, \beta_{dol})$ quantifies the expected excess return associated with exposure to one of the three orthogonal sources of variation in forward premia (the cross-currency, cross-time-and-currency, and cross-time dimensions) each corresponding trading portfolio isolates those components empirically. In this sense, moving from portfolio-based decompositions to regression-based elasticities provides a direct econometric mapping between theoretical trading payoffs and statistical evidence of the UIP.

3.1 From Components to a Spot-Only Carry Specification

In the context of this analysis, we work within a bilateral framework where trading operations are supposed to be funded in US dollars and invested in Uruguayan pesos. Since the forward premium trade loads on the dollar component and the carry trade loads mainly on the static component, I focus on the static trade, which is consistent with the assumption of constant funding at US rates. This framework aligns with the scheme we aim to analyze, given that sharp depreciations of the Uruguayan peso must originate from funding in dollars and investing in pesos.

Since the Uruguayan foreign exchange market is primarily spot-driven, I derive the anomaly specification by replacing the forward premium with the observable interest rate differential using Covered Interest Parity (CIP), focusing on the static elasticity. Using the identity $r_{x,t+1} = (i_t - i_t^*) - \Delta s_{t+1}$, the coefficient in a regression of the depreciation rate on the interest rate differential measures the extent to which the average rate differential is offset by expected depreciation, thereby quantifying the static component of the UIP deviation.

Given the static specification proposed by Hassan and Mano, at the currency level i, the relationship between the excess return on currency i and the global average return can be expressed as (7). I make two key assumptions to adapt this framework to the bilateral case. First, I assume that the expected forward premium approximates the interest rate differential through Covered Interest Parity:

$$fp_i^e \approx (i_t - i_t^*),$$

where i_t and i_t^* represent the domestic (UYU) and foreign (US) interest rates, respectively.[1]

Second, we define the excess return for the average global currency as:

$$r_{x,t+1} = fp^e - \Delta \bar{s}_{t+1},$$

where $\Delta \bar{s}_{t+1}$ denotes the depreciation rate of the average global currency. This expression mirrors the standard excess return definition but applied to the global benchmark.

Substituting these definitions into the static component of the Hassan and Mano specification:

$$r_{xi,t+1} - r_{x,t+1} = \beta_{\text{stat}}\left(fp_i^e - fp^e\right) + \varepsilon^i_{\text{stat},t+1}, \tag{10}$$

[1] In the bilateral setting, the unconditional expectation in the Hassan and Mano static specification is evaluated at time t because the relevant excess return pertains to the full depreciation between t and t+1. Since the payoff is realized over this one-period window, the unconditional component collapses to the information available at time t, preserving the logic and interpretation of the original mapping.

we obtain

$$\big((i_t - i_t^*) - \Delta s_{i,t+1}\big) - \big(fp^e - \Delta \bar{s}_{t+1}\big) = \beta_{\text{stat}}\big((i_t - i_t^*) - fp^e\big) + \varepsilon^i_{\text{stat},t+1}. \tag{11}$$

Rearranging terms to isolate the change in the spot exchange rate,

$$-\Delta s_{i,t+1} = \big(fp^e - (i_t - i_t^*)\big) + \beta_{\text{stat}}\big((i_t - i_t^*) - fp^e\big) - \Delta \bar{s}_{t+1} + \varepsilon^i_{\text{stat},t+1} \tag{12}$$

$$= \big(\beta_{\text{stat}} - 1\big)\big((i_t - i_t^*) - fp^e\big) - \Delta \bar{s}_{t+1} + \varepsilon^i_{\text{stat},t+1}. \tag{13}$$

This equation can be expressed as:

$$\Delta s_{i,t+1} = \big(1 - \beta_{\text{stat}}\big)\big((i_t - i_t^*) - fp^e\big) + \Delta \bar{s}_{t+1} - \varepsilon^i_{\text{stat},t+1}. \tag{14}$$

We now express this as our main spot equation. First, note that the global depreciation factor can be decomposed as:

$$\Delta \bar{s}_{t+1} = \mu_{\bar{s}} + u_{t+1},$$

where $\mu_{\bar{s}}$ is the unconditional mean and u_{t+1} is a zero-mean residual. Under the Hassan–Mano orthogonality assumption, u_{t+1} is uncorrelated with $(i_t - i_t^*)$, ensuring consistent estimation.

Defining $\beta_{\text{spot}} \equiv 1 - \beta_{\text{stat}}$ and $\varepsilon_{t+1} \equiv u_{t+1} - \varepsilon^i_{\text{stat},t+1}$, and grouping constant terms:

$$\alpha \equiv -\beta_{\text{spot}}\, fp^e + \mu_{\bar{s}},$$

we obtain the final estimable specification:

$$\Delta s_{i,t+1} = \alpha + \beta_{\text{spot}}\,(i_t - i_t^*) + \varepsilon_{t+1}. \tag{15}$$

Hence, under these assumptions, the coefficient linking the interest rate differential to expected depreciation in the spot regression, which assess for the excess return of the Uruguayan peso in this case, is $\beta_{\text{spot}} = 1 - \beta_{\text{stat}}$. β_{stat} is the static cross-currency elasticity in the Hassan and Mano framework. In a bilateral, spot-only context with thin forwards, β^{spot} measures how much realized depreciation offsets the interest rate differential driven by persistent carry incentives. In summary, the anomaly underlying the investment strategy to be analyzed rests on the simple fact that, on average, some currencies offer higher currency premia over time than others. This is reasonable if we consider that, for equal expected returns, speculators would choose to invest in the safer currencies [2]. Equation (15) tests whether this anomaly occurs.

Table 1: UIP Spot

	(1) Δs_{t+1}
β_{spot}	-0.0870***
	(0.0308)
α	0.0044***
	(0.0017)
Observations	238
R^2	0.033
Sample period	2020/09/08 to 2025/03/31
$\widehat{\beta}_{stat} = 1 - \widehat{\beta}_{spot}$	1.0870

Standard errors in parentheses
* $p < 0.10$, ** $p < 0.05$, *** $p < 0.01$

The estimated coefficient $\widehat{\beta}_{\text{spot}} = -0.087$ is negative and statistically significant at the 1% level, implying that currencies offering higher interest rates tend, on average, to appreciate rather than depreciate over the subsequent period. This pattern represents a clear deviation from the UIP condition, which would predict $\beta_{\text{spot}} = 1$. In the context of our analysis, such a result indicates that the Uruguayan peso systematically provides a positive excess return when funded in U.S. dollars, consistent with the presence of a persistent currency premium. The corresponding implied static elasticity, $\widehat{\beta}_{\text{stat}} = 1 - \widehat{\beta}_{\text{spot}} = 1.087$, confirms that the cross-currency component dominates the dynamics of expected returns.

Economically, this means that investors engaging in a dollar-funded carry trade into peso-denominated assets were compensated with an excess return that cannot be explained by the simple expectation of depreciation. Instead, it reflects a structural asymmetry between funding and investment currencies, where the peso offers a persistent forward premium that is not offset by future exchange rate adjustments. This reinforces the idea that, during the analyzed period, the Uruguayan peso remained consistently overvalued relative to UIP fundamentals, a finding that aligns with the presence of sustained carry trade incentives.

[2] See e.g. (Lustig et al., 2008) for a broader discussion

3.2 Liquidity Constraints, Speculation, and the Formation of Bubbles

So far, we have set an empirical framework to understand persistent interest rate differential between Uruguayan and the US in the long run, and provided empirical evidence that this is the case for Uruguay. I will now develop how theory explains the mechanisms of sudden depreciations that arise from this anomaly. It is useful to turn to the theoretical framework of Brunnermeier and Pedersen (2008) and Brunnermeier et al. (2009), complemented by the coordination model of Abreu and Brunnermeier (2002).

Brunnermeier and Pedersen (2008) show that speculators play a central role in providing market liquidity by smoothing temporary order imbalances that arise when customers arrive sequentially in the market. In such setting, prices would fluctuate excessively in the absence of speculators, as temporary mismatches between buyers and sellers do not immediately clear. By absorbing these fluctuations generated by sequentiality, speculators effectively provide liquidity (the ease with which an asset can be converted into cash without significantly affecting its price) to the market.

In this framework, speculators are supposed to finance their trades through collateralized borrowing. When purchasing a security, they typically borrow against the asset but must contribute part of their own capital as a margin (or haircut). For instance, if the financier lends only 95% of total capital against the bond, the remaining 5% must be financed with the speculator's own equity. Financiers, such as banks or repurchase-agreement lenders, set these margins to control their Value-at-Risk (VaR) exposure and can adjust them each period.

When volatility rises, whether due to genuine fundamental shocks or temporary liquidity shocks, financiers increase margins to re-set their VaR. This generates funding liquidity risk, since speculators must either supply more capital or liquidate positions. If speculators' capital constraints become binding, they are forced to sell assets to affront obligations, reducing market liquidity and amplifying price declines.

This mechanism creates two reinforcing feedback loops or "liquidity spirals" as identified by Brunnermeier and Pedersen (2008). First a margin spiral, where an initial rise in volatility leads financiers to increase margins, reducing speculators' leverage and forcing asset sales to meet margin calls; these sales depress prices, further increasing volatility and prompting additional margin tightening; and second a loss spiral, where adverse price movements generate mark-to-market losses that erode speculators' capital, forcing further deleveraging and additional sales that, in turn, cause further price declines. Together, these spirals generate nonlinear amplification, where relatively small funding shocks produce disproportionately large market dislocations. Historical examples include the LTCM collapse during the 1998 Russian default and the 2007–2008 subprime crisis, in which relatively moderate initial losses triggered massive liquidity contractions. In contrast, margins can theoretically decrease with illiquidity and thus can be “stabilizing”. This happens when financiers know that prices diverge due to temporary market illiquidity and know that liquidity will be improved shortly.

Given this characterization, it can analyzed how it translates to the foreign exchange rate market. Particularly, what happens in the case of a raise in the domestic interest rate. In a frictionless, risk-neutral economy, UIP would imply an immediate appreciation of the domestic currency, followed by a predictable future depreciation that compensates carry trade profits. Although, Brunnermeier et al. (2009) argue that a sudden rise in the interest rate of an investment currency initially attracts foreign capital, leading to sustained appreciation. This happens because, with liquidity constraints and slow-moving capital, the adjustment is gradual (investment currency stays “appreciated”). After an increase in the interest rates, slight deprecations could be observed due to the increase in volatility that reduced peso-denominated instruments demand, but in the long term speculators continue to hold their positions as long as liquidity remains ample, delaying the correction of overvalued exchange rates. This generates a relation between the interest rate differential and the depreciation like the one stated in Table 1. As in Abreu and Brunnermeier (2002), each speculator knows that a crash will eventually occur but is uncertain when others will exit; hence, coordination failures lead to persistent “bubbles” in exchange rates.

When funding conditions tighten and margins rise, the coordinated unwinding driven by the strategic complementarities of carry positions causes a sudden and sharp depreciation of the investment currency. Brunnermeier et al. (2009) emphasize that increases in margins act as a coordination device: once margins rise, all leveraged investors simultaneously find their positions more expensive to maintain, which forces them to reduce leverage at the same time. Even speculators who would otherwise prefer to remain invested must liquidate positions because they anticipate that others will do so as well. This mechanism is perfectly aligned with the global-game structure of Abreu and Brunnermeier (2002), where arbitrageurs know that a correction is inevitable but face uncertainty about the timing of others’ exits. A rise in margins therefore serves as a public signal that shifts beliefs about when others will unwind. Once a critical threshold is crossed, expectations coordinate on immediate liquidation, triggering a synchronized exit and generating the abrupt, crash-like depreciation characteristic of carry trade unwinding episodes.

In a setting like the one described above, a timely Central Bank intervention would be optimal to counteract this form of liquidity stress, since individual agents fail to internalize the externalities associated with the loss spiral triggered by their sales. By providing liquidity when funding conditions tighten, the Central Bank can possibly dampen these feedback effects, prevent excessive exchange rate depreciations, and restore market stability.

4 Identification

In the previous section, I established which dimension of the UIP anomaly is required for the profitability of carry trade operations and provided empirical evidence that this anomaly is present in the Uruguayan economy. This allows me to test the main hypothesis of this work: that carry trade operations drive exchange rate dynamics. The question to answer is: do increases in carry trade incentives generate higher demand for LRMs?

To test the main hypothesis, the first step is to characterize exchange rate dynamics during the period and to build a GARCH model in which the interest rate differential plays a significant role. This will test the hypothesis that the interest rate differential negatively affects both the mean and the volatility of the exchange rate. Subsequently, using the conditional volatility derived from the model (assumed to be known by agents based on the information available up to time t), the CTR is constructed as a proxy for carry trade incentives. Finally, to assess whether exchange rate dynamics are driven by carry trade activity, I conduct local projections of the CTR on the demand for LRMs.

4.1 Data

All variables are expressed as weekly averages of daily observations to ensure a common frequency and reduce day–of–week effects.

- Interest rates. The overnight call rate for Uruguay is sourced from EconUY (econuy.com). US Treasury rates are retrieved from the Federal Reserve Bank of St. Louis (FRED). These series are used to build the short-term interest–rate differential in weekly averages, $i_t - i_t^*$.

- Exchange rate. The bilateral USD/UYU series is obtained from EconUY, and corresponds to the interbank market sell rate. It is converted to weekly averages. I work with $s_t = \log(\text{USD}/\text{UYU}_t)$ and $\Delta s_{t+1} = s_{t+1} - s_t$.

- Monetary Regulation Bills. Proposed amount for purchases of LRMs (proxy for evidence of carry trade activity) is obtained from the Bolsa Electrónica de Valores (BEVSA). I organize these data by maturity buckets of 1–60, 60–120, and > 120 days. I work with the logarithm of totals by week. The series are smoothed using a four-week moving average.

4.2 Exchange Rate Dynamics

4.2.1 Distributional Properties of Exchange Rate

To start characterizing the USD/UYU exchange rate behavior, I study the higher-order properties of the distribution of its weekly returns. Let $\Delta s_t = \Delta \log(\text{USD/UYU})_t$ denote the weekly log change in the exchange rate. The skewness and kurtosis of Δs_t are defined as:

$$\text{Skew}(\Delta s_t) = \frac{E[(\Delta s_t - \mu)^3]}{\sigma^3}, \tag{16}$$

$$\text{Kurtosis}(\Delta s_t) = \frac{E[(\Delta s_t - \mu)^4]}{\sigma^4}, \tag{17}$$

where $\mu = E[\Delta s_t]$ and $\sigma^2 = Var(\Delta s_t)$.

Skewness measures the relative weight of the tails of the distribution. A positive skewness implies that large positive returns are more likely than large negative ones. Since $r_t = \Delta \log(\text{USD/UYU})_t$, positive values correspond to depreciations of the peso. Therefore, a positive skewness indicates that large depreciations tend to be more pronounced than large appreciations. Kurtosis measures the fatness of the tails relative to a Gaussian benchmark, with values greater than 3 indicating a higher probability of extreme movements.

Table 2 reports the sample skewness and kurtosis for the exchange rate returns in the period under study.

Statistic	Value
Skewness	0.39
Kurtosis	4.43
Observations	235
Sample period	2020/09/01 to 2025/03/31

Table 2: Skewness and kurtosis of weekly exchange rate returns $\Delta \log(\text{USD/UYU})$.

The positive skewness indicates that appreciations of the peso tend to be gradual, while depreciations are more abrupt. This feature is consistent with an exchange rate dynamic influenced by carry trade operations: during periods of high interest rate differentials, speculative inflows contribute to a slow appreciation of the peso, whereas unwind episodes lead to large and sudden depreciations. The excess kurtosis reflects fat tails, implying that extreme exchange rate movements occur more frequently than under a Gaussian benchmark, which could also be responding to carry dynamics.

Figure 1 compares the empirical kernel density of returns with a fitted normal density. The empirical distribution exhibits a sharper peak and heavier tails relative to the normal benchmark, consistent with the kurtosis estimate. Moreover, the right tail is visibly more pronounced, in line with the positive skewness estimate.

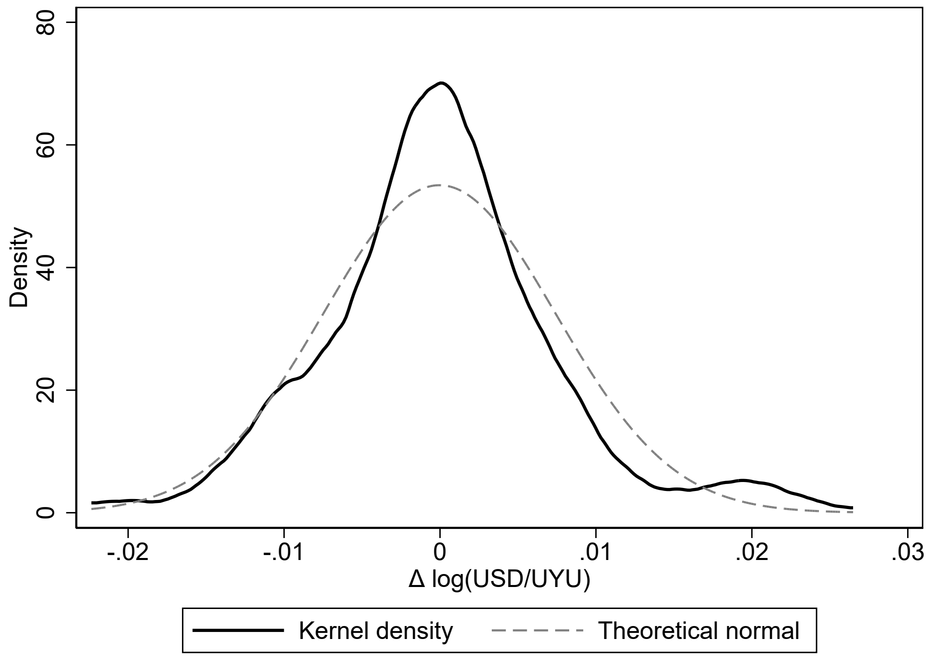

Figure 1: Kernel density of weekly exchange rate returns vs. fitted normal distribution.

Sample period: 2020/09/01 to 2025/03/31. Source: own elaboration.

Figure 2 shows a Q–Q plot of the empirical distribution against the quantiles of the normal distribution. The upward deviation of the upper quantiles indicates a heavier right tail, implying that large depreciations of the peso are more likely than predicted by a Gaussian benchmark.

These distributional properties provide important information for the interpretation of the mean and volatility dynamics estimated previously. They show evidence supporting that gradual appreciations correspond to the left side of the distribution, where returns cluster around small negative values and volatility remains low. In contrast, unwind episodes correspond to the heavy right tail of the distribution. Thus, the positive skewness is consistent with a regime in which appreciations are accompanied by lower volatility, reflecting carry trade compression, while the possibility of sudden and sharp depreciations remains present.

These distributional asymmetries are consistent with the mechanism described in Section 3, whereby higher interest rate differentials attract speculative inflows that gradually appreciate the peso and compress volatility. However, these conditions coexist with the risk of abrupt reversals, consistent with the crash-risk view of carry trade dynamics.

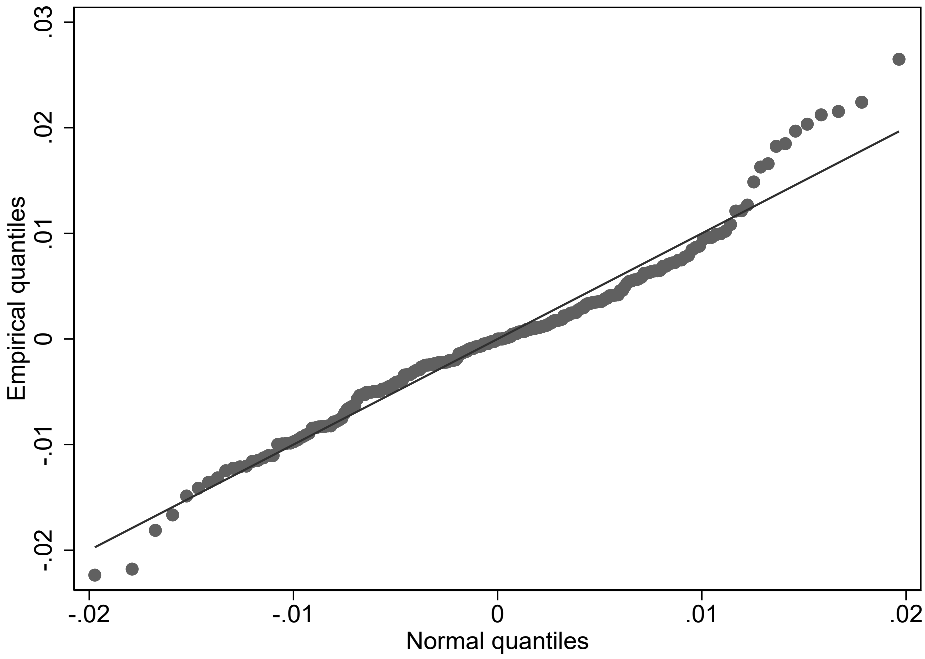

Figure 2: Q–Q plot of exchange rate returns relative to a normal distribution.

Sample period: 2020/09/01 to 2025/03/31. Source: own elaboration.

4.2.2 GARCH Model

This subsection aims to model the weekly USD/UYU process during the period, identifying its mean and conditional variance dynamics with a GARCH model, in line with the stylized facts for exchange rate returns (Hsieh, 1989). As mentioned, the model will involve the interest rate differential as the main variable. The underlying idea is that the dynamics characterized in the previous subsection may be related to the interest rate differential. In the data, this pattern can be observed in Figures 3 and 4, where periods of wider differentials with the U.S. coincide with both a lower average level of the exchange rate and a reduced conditional variance.[3] For example, observing Figure 3, we can see that periods like the one between April and October 2023, characterized by a higher interest rate differential, lead to a standardized exchange rate mean below its average during the period. Also, analyzing Figure 4, we observe that fluctuations in the exchange rate tend to be smoother (and mainly negative) when interest rate differentials are higher.

By including the interest rate differential in the mean equation of the exchange rate return within the GARCH model, the conditional variance σ^2_{t+1} becomes linked to the interest rate differential through two channels. First, it depends directly on recent exchange rate movements and their deviations from the

[3]Given our rolling-window estimations of conditional variance, the final period of estimation spans from 07/02/2023 to 31/03/2025.

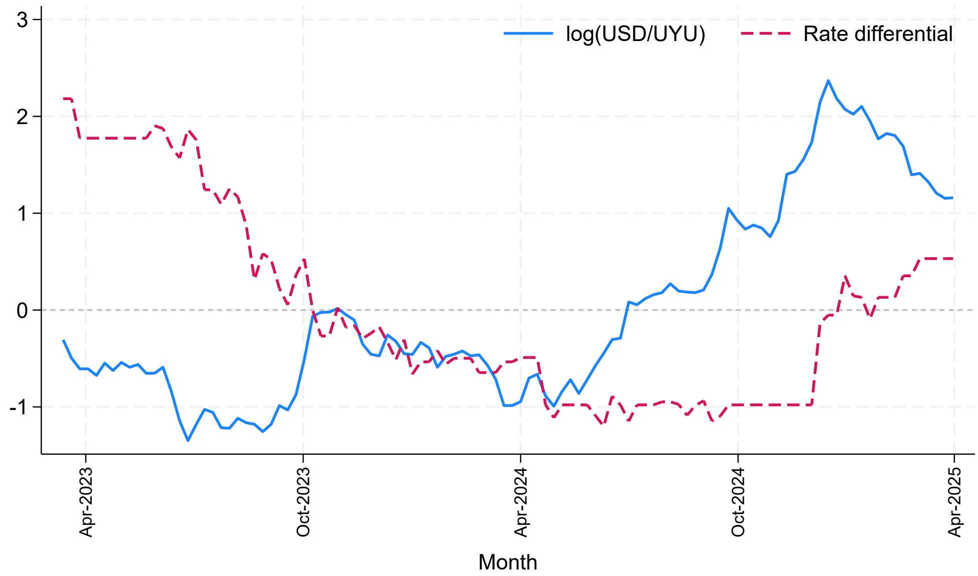

Figure 3: Rate differential vs. log(USD/UYU), both standardized (weekly).

Source: own elaboration.

mean, as in any GARCH process. Second, it depends indirectly on the interest rate differential, because higher differentials are associated with exchange rate appreciations—which, as shown in the previous subsection, tend to occur in periods of lower volatility. Thus, the interest rate differential influences both the conditional mean and, indirectly, the conditional variance of exchange rate returns.

Unit–root diagnostics employs ADF tests on s_t (with intercept) and on Δs_t (without intercept). The ADF augmentation lag is chosen according to the Schwert (1989) rule,

$$L = \left\lfloor 4\,(N/100)^{1/4} \right\rfloor, \tag{18}$$

with N denoting the sample size. For the period spanning September 1, 2020 to March 31, 2025, the exchange rate in levels behaves as an I(1) process: the null hypothesis of a unit root is rejected for the first difference but not for the level series, with rejections occurring at all conventional significance levels. The interest rate differential also exhibits non-stationarity in levels, with the ADF test failing to reject the unit-root null; however, the unit-root hypothesis is rejected for the first difference at all conventional significance levels, confirming stationarity in the differenced series. Accordingly, both variables are taken in first differences in the subsequent modeling to ensure stationarity.

To justify the use of a GARCH specification, I first assess whether the residuals from a homoskedastic model exhibit autoregressive conditional heteroskedasticity. Specifically, the mean equation in (19) is estimated under the assumption of constant variance, and the resulting residuals $\hat{\varepsilon}_t$ are obtained. Sub-

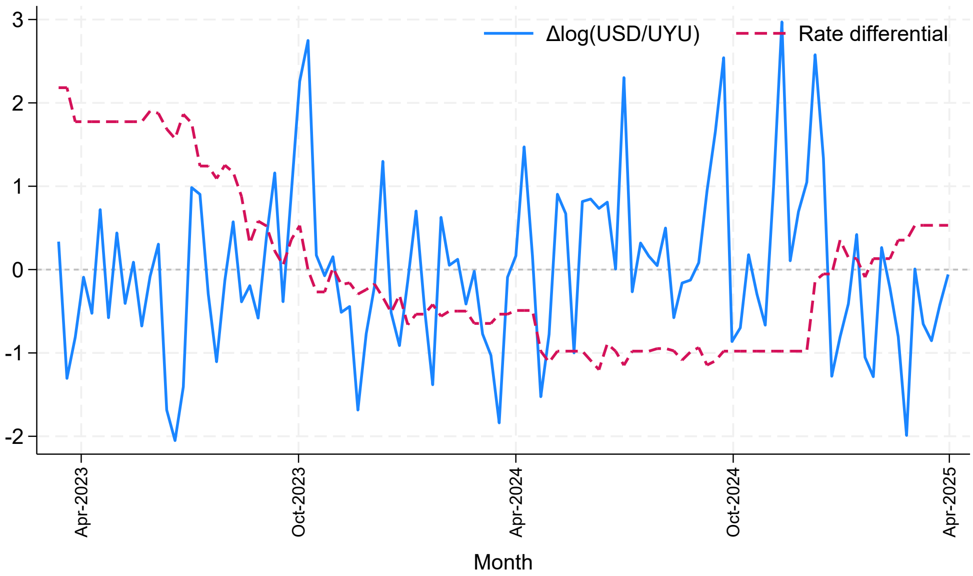

Figure 4: Rate differential vs. Δlog(USD/UYU), both standardized (weekly).

Source: own elaboration.

sequently, the ARCH–LM tests of Engle (1982) are applied to $\hat{\varepsilon}_t^2$ to detect whether current volatility depends on past squared innovations. Under the null of no ARCH effects, $\mathrm{Var}(\varepsilon_{t+1} \mid \mathscr{F}_t)$ is constant over time; rejection implies that volatility is time-varying and predictable based on past shocks. In our case, the null is rejected at all conventional significance levels for lags between 1 and 8, supporting the presence of conditional heteroskedasticity and the pertinence of a GARCH-type model.

Intuitively, GARCH effects arise when large deviations from the mean tend to cluster: periods of high volatility are followed by high volatility, and calm periods are followed by calm periods. Even though the innovations ε_t have mean zero by construction, their variance evolves depending on past price movements. This behavior is central in the context of speculative carry operations, since risk is not only related to the expected depreciation but also to the conditional scale of fluctuations experienced in short horizons.

To characterize correctly exchange rate dynamics (and to obtain $\widehat{\sigma}_{t+h|t}$ for (21)), the chosen specification is a GARCH(1,1) model, which results are shown in Table 2. An event dummy is included on 26 Dec 2022 to absorb transient disturbances:

$$\Delta s_{t+1} = \phi_1 \Delta s_t + \phi_4 \Delta s_{t-3} + \beta_{\text{dif}} \Delta(i - i^*)_{t-2} + \delta \mathbf{D}_t + \varepsilon_{t+1}, \tag{19}$$

$$\varepsilon_{t+1} \mid \mathscr{F}_t \sim (0, h_{t+1}), \quad h_{t+1} = \omega + \alpha\, \varepsilon_t^2 + \beta\, h_t. \tag{20}$$

I estimate a mean equation that is ARX with lags 1 and 4 of Δs_t and no intercept, including $\Delta(i_t - i_t^*)$ at $t-2$ and event dummies. The variance follows a GARCH(1,1) with one lag of the squared innovation ε_t^2 and one lag of the conditional variance h_t. $\mathbf{D}_t$ includes the event dummy corresponding to the Central Bank's implicit announcement that it was ending its cycle of interest rate hikes—after raising the policy rate to 11.5%—in a context of declining inflation. This signal of a policy shift, combined with year-end market factors, altered the dollar's trend during the last week of December. The ARCH and GARCH parameters remain statistically significant and $\alpha + \beta \approx 0.82 < 1$, indicating a stationary yet persistent volatility process. Therefore, the GARCH(1,1) specification remains adequate for modeling conditional variance and generating forward-looking volatility estimates.

Diagnostic checks on standardized residuals z_t are performed to ensure that the GARCH(1,1) specification adequately captures volatility dynamics. Ljung–Box Q-tests applied to the standardized residuals z_t indicate no evidence of autocorrelation when considering up to 4 lags. Same test applied to the squared residuals z_t^2 does not suggest remaining autocorrelation in the variance, confirming that the GARCH specification successfully captures volatility clustering. Therefore, the GARCH(1,1) specification remains adequate for modeling conditional variance and generating forward-looking volatility estimates.

Table 3: GARCH(1,1) model for Δs_t

Mean	
	Δs_t
AR(1)	0.3057***
	(0.0640)
AR(4)	0.1555***
	(0.0556)
β_{dif} (t-3)	-0.0036**
	(0.0014)
Dummy: 26 Dec 2022	0.0276***
	(0.0066)
Volatility	
α	0.3449***
	(0.1178)
β	0.4921***
	(0.1424)
Observations	234
Sample period	2020-10-12 to 2025-03-31

Standard errors in parentheses

* $p < 0.10$, ** $p < 0.05$, *** $p < 0.01$

The estimated coefficient of -0.0036 for $\beta_{\text{dif}}(t-3)$ implies that a 100-basis-point increase in the interest rate differential from one week to the next leads to an appreciation of approximately 0.36% in the exchange rate three weeks later. This result confirms the initial hypothesis that higher interest rate differentials are correlated with both a lower conditional mean and a lower conditional variance of the exchange rate. The delayed response suggests that monetary policy transmission operates with a lag of about three weeks in currency markets. Both volatility components display significant persistence: the ARCH term ($\alpha = 0.345$) indicates that 34.5% of shock-induced volatility carries over to the next period, while the GARCH term ($\beta = 0.492$) shows that 49.2% of the current conditional variance persists into future volatility. The combined persistence ($\alpha + \beta = 0.837 < 1$) suggests a stationary yet highly persistent volatility process, implying that exchange rate uncertainty exhibits strong momentum over time.

4.3 Carry to Risk Ratio

Given that carry trade activity is difficult to measure directly—since it would require detailed investor-level position data, which are rarely available—the next step is to construct an indicator that approximates carry trade incentives. This allows me to empirically assess the effects on variables of interest when such incentives are relatively high. For this purpose, I use the well-known carry–to–risk ratio, originally proposed by Curcuru et al. (2010) and applied to Latin American cases in Díaz et al. (2013) and Gamboa-Estrada (2016). This indicator summarizes both the potential payoff (interest rate differential) and the associated risk (exchange rate volatility), making it an appropriate measure of conditions favorable to carry trade activity. The contribution of this work relative to previous studies is the construction of a forward-looking, dynamically reinforced CTR: instead of relying on unconditional or static measures of volatility, I use the GARCH-implied conditional variance of the exchange rate based solely on information available at the time the position is taken.

Introducing the interest rate differential into the GARCH model that generates the conditional volatilities allows the specification to capture the non-linear effects associated with carry trade dynamics (see Section 4.2.2). Since the response variable is the first difference of the logarithm of the exchange rate, a negative coefficient on the differential implies a lower expected depreciation of the investment currency. This increases carry trade incentives not only through its direct impact on exchange rate returns, but also through its association with lower conditional volatility. These periods of relative “calm” attract additional speculative inflows, further appreciating the investment currency and reinforcing the initial effect. This methodological approach captures the dynamic interaction between interest rate differentials, volatility, and self-reinforcing inflows more precisely than approaches based solely on unconditional volatility or static spread levels.

Following the modeling of conditional volatility in Section 3.2, I define a horizon–h carry–to–risk ratio that scales the payoff by model-implied risk:

$$\mathrm{CTR}_t^{(h)} = \frac{i_t - i_t^*}{\widehat{\sigma}_{t+h|t}}, \qquad h \in \{4, 13, 46\} \text{ weeks}, \tag{21}$$

where $\widehat{\sigma}_{t+h|t}$ is the forecast standard deviation of $\sum_{j=1}^{h} \Delta s_{t+j}$ based on information available at time t. Each investor evaluates risk over the horizon during which she is exposed to potential sudden depreciations, so the relevant volatility forecast depends on h. The chosen horizons correspond to the average duration of operations within each LRM maturity bucket. Intuitively, longer-term operations tend to exhibit lower CTRs because conditional volatility converges toward the unconditional variance of the GARCH model, $\omega/(1-\alpha-\beta)$, reducing short-term gains from volatility compression. The distinction across horizons allows us to examine meaningful differences across maturity buckets in the Uruguayan market. The numerator in (21), the interest rate differential, approximates the yield on Monetary Regulation Bills in Uruguay and on U.S. Treasury securities, which are the main instruments underlying carry trade operations (BIS, 2015; Fernández et al., 2023). Since the selected policy rates ultimately determine the pricing of these instruments, the differential accurately captures the return component of the carry trade operation.

To reproduce agent-based decision making at each point in time, rolling dynamic volatility forecasts are estimated for $h \in \{4, 13, 46\}$ weeks by re-estimating the model over expanding windows and predicting $h_{t+h|t}$. The square roots yield $\widehat{\sigma}_{t+h|t}$ used in (21). This ensures that the CTR at time t reflects forward-looking risk over the relevant horizons (approximately one, three, and eleven months). The rolling estimation begins with 132 observations, so CTR values are available from 13/03/2023 to 31/03/2025.[4] Estimates of the different CTRs are shown in Figure 3. As expected, longer-horizon CTRs are lower because volatility converges to its unconditional mean, while short-term CTRs spike in periods of low conditional variance.

By incorporating the joint behavior of the interest rate differential, volatility, and the exchange rate mean, the CTR constructed here provides a more accurate approximation of carry trade incentives. Essentially, the goal is to capture the non-linear dynamics characteristic of carry trades, grounded in the theoretical framework and supported by the data: appreciations tend to be mild and sustained, whereas when market conditions reverse, incentives deteriorate sharply due to margin and loss spirals, leading to rapid unwinding of peso positions and sudden depreciations of the exchange rate.

[4]The choice of 132 initial observations ensures a complete response-variable grid for all horizons considered in the construction of the CTR series.

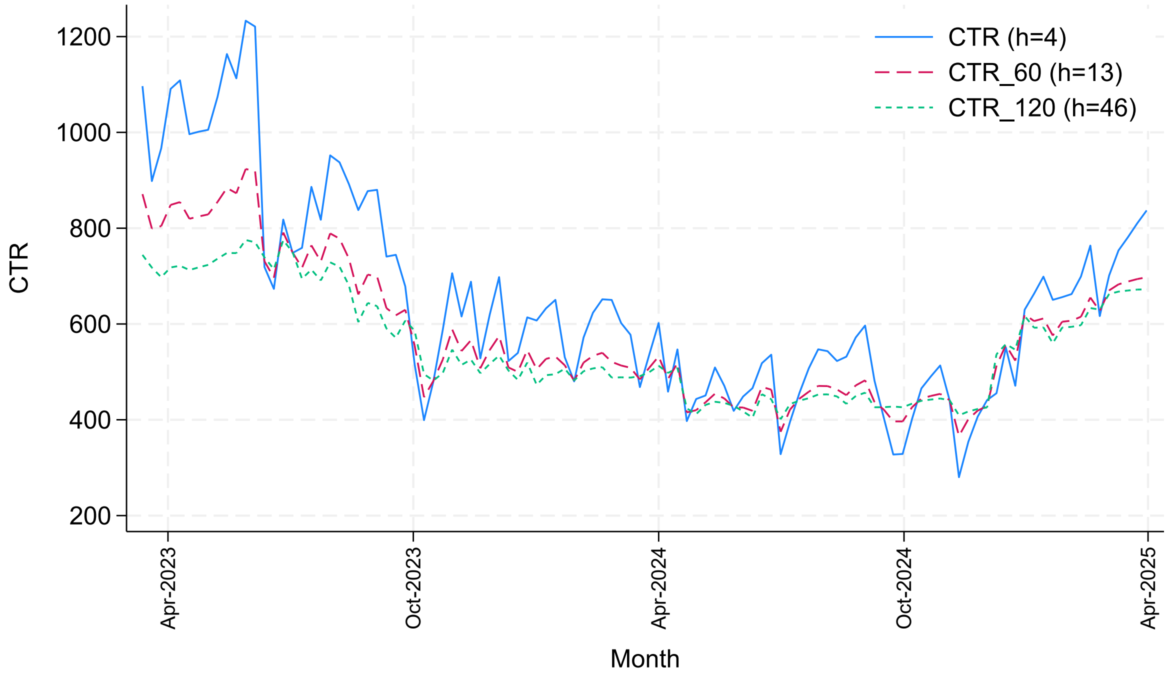

Figure 5: Evolution of Carry-to-Risk ratios for horizons $h = 4$, $h = 13$, and $h = 46$ weeks.

Source: own elaboration.

4.4 CTR and LRM relation

This final step evaluates whether carry is indeed a significant channel driving exchange rate dynamics. In other words, it allows us to assess, with empirical evidence, whether the relationships found in Step 1 between the interest rate differential and exchange rate dynamics are attributable to carry trade activity.

Using impulse-response local projections, I test whether a higher CTR translates into a greater demand for LRMs. This instrument is used as a proxy for carry trade activity, since it is the primary funding asset for currency carry trades. Monetary Regulation Bills offer an attractive option for investors seeking to profit from interest rate differentials, as they provide short-term returns without direct exposure to the risks associated with more volatile assets. Using the proposed amount of LRMs purchase as the dependent variable provides a close approximation to the actual demand for these instruments in the market.

To measure how these instruments react to carry incentives, I estimate local projections at horizons $h = 0, \dots, H$. I set $H = 4$ weeks, so the estimated responses capture changes in LRM demand over roughly one month after a change in incentives. There is a trade-off between extending the horizon to analyze longer-term responses to a 100-basis-point CTR increase and maintaining reasonable standard errors. Nevertheless, the most significant effects are expected to appear within the first or second week following the increase in CTR. Additional specifications estimated for robustness are presented in Appendix B. Newey–West standard errors are used with bandwidth h to account for overlapping-horizon serial correlation.

Let $y_t^{(m)} = \log(\mathrm{LRM}_t^{(m)})$ denote the weekly four-week moving average logarithm of the proposed amount for maturity bucket m. The local projections are specified as:

$$\Delta y_{t\to t+h}^{(m)} = a_h^{(m)} + \sum_{\ell=1}^{p} \psi_{h,\ell}^{(m)} \Delta y_{t+1-\ell}^{(m)} + \sum_{\ell=0}^{p} \kappa_{h,\ell}^{(m)} \Delta \mathrm{CTR}_{t-\ell}^{(m)} + v_{t+h}^{(m)}, \tag{22}$$

with $p = 2$ lags for persistence control. I display point estimates for $\kappa_{h,\cdot}^{(m)}$ with 90% confidence bands (± 1.645 SE). Cumulative responses reflect:

$$\sum_{j=0}^{h} \widehat{\kappa}_{j,0}^{(m)},$$

that is, the sum of the horizon-j contemporaneous coefficients ($\ell = 0$). Presenting both level–by–level responses and their cumulative counterpart helps distinguish temporary spikes from persistent shifts in demand.

Confidence bands reflect the estimation uncertainty of each coefficient $\hat{\beta}_h$ individually and are useful for visualizing sampling variability at each horizon. However, as noted by Inoue et al. (2023), these point-wise intervals cannot be used to test whether the entire sequence of responses jointly differs from zero. For that purpose, significance bands provide a more appropriate graphical representation of the null hypothesis $H_0 : \beta_0 = \beta_1 = \ldots = \beta_H = 0$, namely that the treatment has no effect at any horizon.

It is important to note that the demand for these peso-denominated bills is also influenced by other actors unrelated to carry-trade activity, such as pension fund administrators, whose portfolio decisions are largely independent of the variables driving carry-trade incentives. Therefore, the significant effects we identify occur despite this rigidity in demand contributed by non-carry participants.

The use of local projections is key for this analysis, as it allows us to trace how the effect of an increase in the indicator unfolds over time on the demand for peso-denominated instruments. This decomposition enables us to examine whether the dynamics follow the mechanism proposed by Brunnermeier et al. (2009), in which small initial depreciations are followed by gradual appreciations that persist over time, since separate regressions are estimated to measure the impact at each horizon.

If, for example, a VAR specification were used instead, a common lag structure would be imposed. Although more efficient under correct specification, such a framework would prevent us from capturing the detailed dynamics of interest. The trade-off with local projections is that they produce larger standard errors for the estimated coefficients, but reduce bias.

5 Carry Trade Effects on LRM Demand

Figures in this section display the response of LRMs to a 100-basis-point increase in the corresponding CTR, estimated through local projections following Jordà (2005). The blue lines represent the point estimates of the impulse response at each horizon, while the gray and orange shaded areas correspond to 90-percent point-wise confidence bands and 90-percent joint significance bands, respectively.

Under this approach, I analyze the results as follows: if the entire impulse response lies within the orange band, the null of no effect cannot be rejected; conversely, if the blue line exits the band at any horizon, the null is rejected, indicating that the shock produces a statistically significant effect in at least one period (Inoue et al., 2023, p. 7). From a methodological standpoint, this illustrates the advantage of combining the local-projection framework of Jordà (2005) with the joint-inference visualization proposed by Inoue et al. (2023). While confidence bands convey uncertainty for each coefficient individually, significance bands summarize the outcome of a joint hypothesis test, analogous to an F-test in a system of equations.

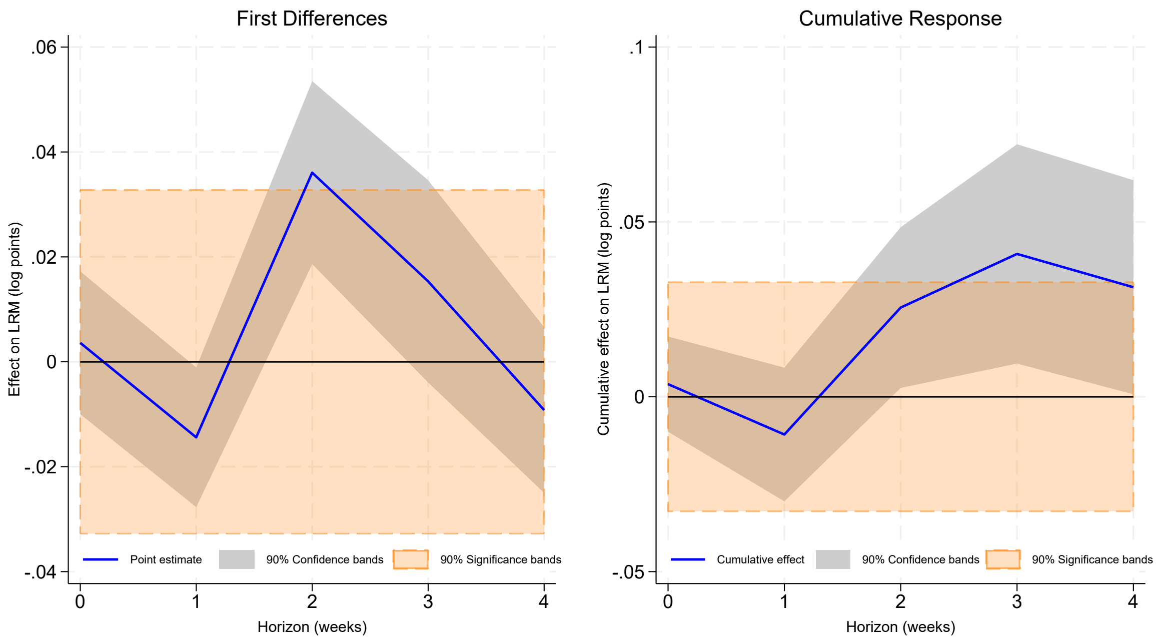

Gray: 90% point-wise confidence bands, Orange: 90% joint significance bands (Bonferroni-adjusted)

Figure 6: Response of LRM (1–60 days) to a 100-point increase in CTR_4.

Source: own elaboration.

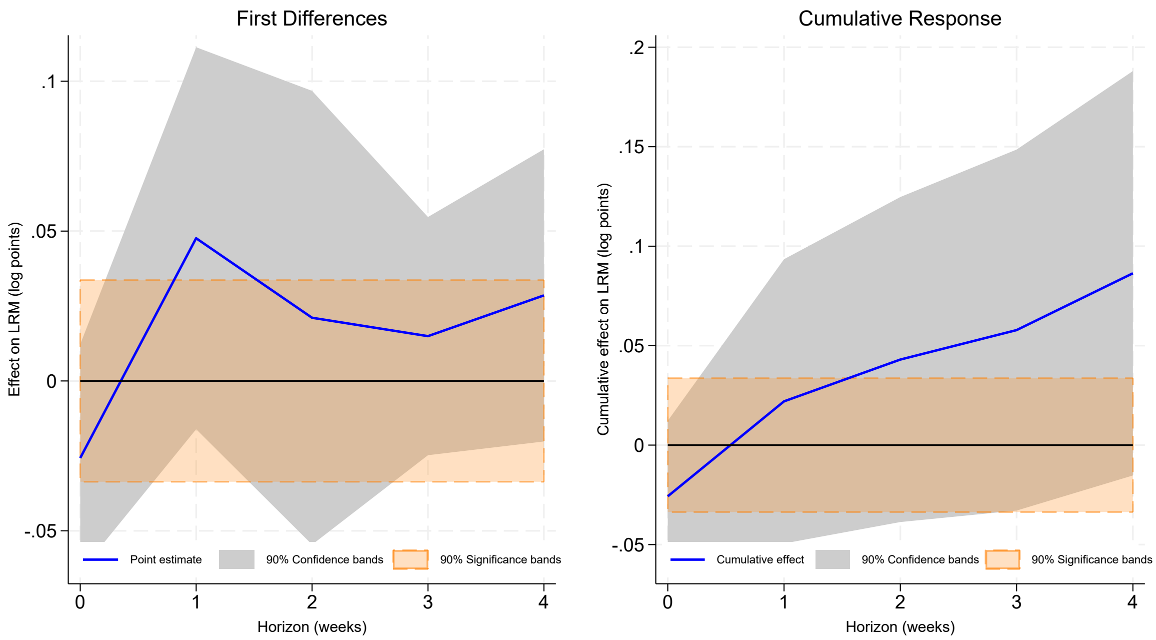

Gray: 90% point-wise confidence bands, Orange: 90% joint significance bands (Bonferroni-adjusted)

Figure 7: Response of LRM (60–120 days) to a 100-point increase in CTR_{13}.

Source: own elaboration.

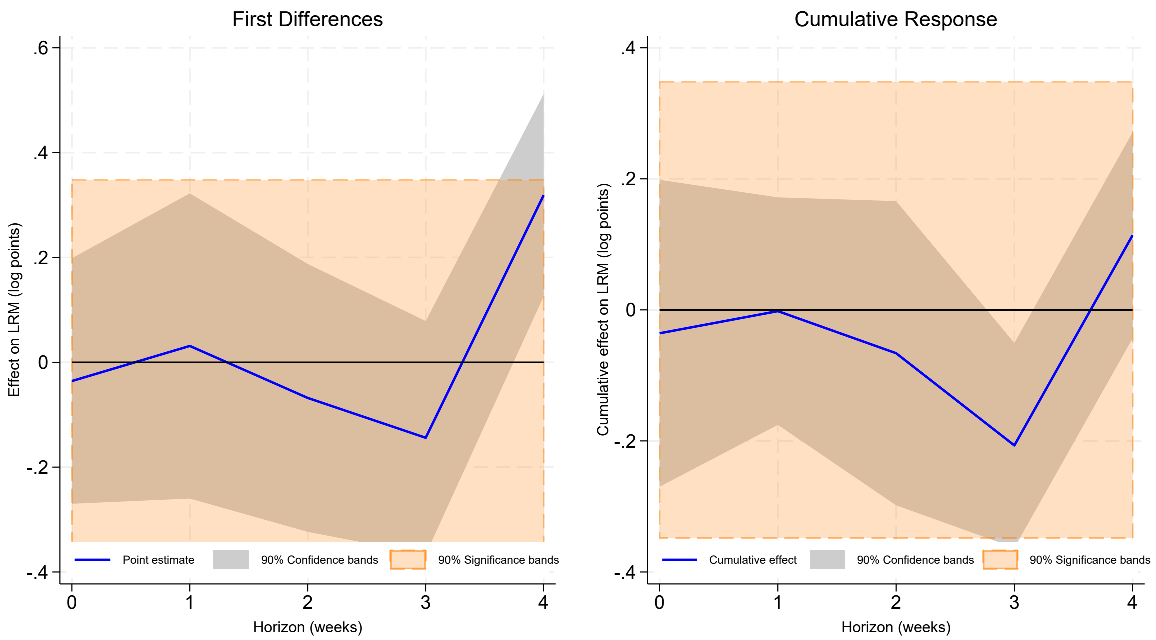

Gray: 90% point-wise confidence bands, Orange: 90% joint significance bands (Bonferroni-adjusted)

Figure 8: Response of LRM (120+ days) to a 100-point increase in CTR_{46}.

Source: own elaboration.

For the 1–60 day maturity segment (Figure 6), the response becomes positive in the first week after the shock, with the point estimate peaking around 0.02 log points before declining. This delayed reaction reflects that carry trade incentives take some time to translate into actual demand. The pattern may also reflect that this bucket includes instruments of less than 30 days, which are generally unrelated to carry trade activity, thereby weakening the contemporaneous response. Moreover, given the short duration of certain operations, some positions may be partially unwound by the third week, contributing to the modest negative (although not significant) effect thereafter. Despite these complexities, the cumulative effect remains positive and significant, indicating an overall increase in demand for the Uruguayan currency following a rise in CTR.

For the 60–120 day maturity segment (Figure 7)—where the bulk of carry trade activity occurs according to BIS (2015)—the response matches the theoretical prediction: delayed but cumulatively significant increase in demand. The effect peaks at approximately 0.05 log points (around a 5 percent increase in LRM demand) and remains positive across horizons. In both the difference and cumulative specifications, the response exits the joint significance bands, confirming statistical significance. The cumulative response exhibits a steadily increasing trajectory, suggesting a persistent effect of CTR shocks on LRM demand over roughly four weeks, validating dynamics suggested theoretically.

For the longest maturity bucket (120+ days; Figure 8), with an average duration of about 42 weeks, no statistically significant response is detected. This aligns with theoretical expectations, since carry trade positions are rarely held over such long horizons due to elevated depreciation risk. Moreover, for these maturities, expectations about future interest rates play a central role—a dimension not captured in our empirical strategy, which focuses on short-term operations where the interest rate differential is more predictable.

Robustness checks using specifications with one and three lags of both the dependent and independent variables show that the main results are preserved for the 0–60 and 60–120 day buckets under the three-lag specification, although they weaken under the one-lag alternative. The 120-plus bucket remains statistically insignificant across all specifications. The dynamics of the impulse response closely mirror those obtained in the baseline model. This reinforces the interpretation that the carry trade mechanism is the driving force behind the estimated effects, since the results remain robust to an alternative specification precisely in the maturity segments most exposed to carry trade activity and the dynamic patterns continue to align with the theoretical predictions.

Overall, I find evidence that increases in carry trade incentives lead to higher demand for peso-denominated instruments in the 1–60 and 60–120 day maturity segments. Therefore, there is significant evidence to answer the research question guiding this study: an increase in carry trade incentives generates greater demand for peso-denominated Monetary Regulation Bills. This implies that there is evidence supporting the central hypothesis of this study: carry trade operations are an significant driver of exchange rate dynamics in Uruguay. The evidence is further reinforced by the fact that the strongest effects arise in the maturity segments where carry trade activity is most prevalent, and that the transmission patterns closely align with theoretical predictions.

6 Conclusions

This thesis provides empirical evidence on three key mechanisms governing exchange rate dynamics in Uruguay, with relevant implications for economic policy design. First, the interest rate differential between Uruguay and the United States exerts a statistically significant influence on both the level and volatility of the exchange rate. The estimated GARCH models demonstrate that a higher differential is directly associated with a lower mean depreciation of the Uruguayan peso, and indirectly reduces exchange rate volatility through its correlation with exchange rate appreciations that, as shown by the skewness and kurtosis analysis in Section 4.2.1, present a distribution with lower variance.

Second, by analyzing a specific channel through which the carry trade operates, I confirm the hypothesis that carry trade incentives generate persistent demands for local currency that create conditions conducive to rational bubble formation in asset prices. The evidence in Section 3.3 shows that our proxy for carry trade activity increases when CTR rises, particularly in the 1-60 and 60-120 day maturity segments where these operations are most prevalent. The delayed response patterns align with theoretical predictions of coordinated speculation dynamics.

Third, and relevant for economic policy, the empirical evidence supports the view that carry trade operations have shaped exchange rate dynamics during the analyzed period. This implies that, once the coordination mechanism described by Abreu and Brunnermeier (2002) is triggered - interpreted here through increases in carry trade incentives - speculators may withdraw abruptly when conditions change. From a policy perspective, this suggests that intervention may be optimal during such episodes. Individual investors do not internalize the systemic costs of the loss spiral that is triggered when they unwind their positions, which in turn induces other agents to do the same. Consequently, intervention at that critical point could prevent the loss spiral and preserve exchange rate stability.

References

Abreu, D. and Brunnermeier, M. K. (2002). Synchronization risk and delayed arbitrage. *Journal of Financial Economics*, 66(2–3):341–360.

BIS (2015). Currency carry trades in latin america. Bis papers no. 81, Bank for International Settlements, Basel. Report submitted by a Study Group established by the Consultative Group of Directors of Operations in the Americas Region and chaired by Julio A. Santaella, Bank of Mexico.

Brunnermeier, M. K., Nagel, S., and Pedersen, L. H. (2009). Carry trades and currency crashes. pages 313–347.

Brunnermeier, M. K. and Pedersen, L. H. (2008). Market liquidity and funding liquidity. *The Review of Financial Studies*, 22(6):2201–2238. FS Advance Access published December 10, 2008.

Burnside, C., Eichenbaum, M., Kleshchelski, I., and Rebelo, S. (2011). Do peso problems explain the returns to the carry trade? *Review of Financial Studies*, 24(3):853–891.

Carreño, J. and Cox, P. (2014). Carry trade y turbulencias cambiarias con el peso chileno. Documentos de Trabajo 733, Banco Central de Chile, Santiago, Chile.

Curcuru, S., Vega, C., and Hoek, J. (2010). Measuring carry trade activity. Technical report, Board of Governors of the Federal Reserve System.

Díaz, S. A., González, P. A., and Sotz, C. A. (2013). Carry-to-risk ratio como medida de carry trade. *Economic Statistics Series*, 94.

Engel, C. (1996). The forward discount anomaly and the risk premium: A survey of recent evidence. *Journal of Empirical Finance*, 3(2):123–192.

Engle, R. F. (1982). Autoregressive conditional heteroscedasticity with estimates of the variance of united kingdom inflation. *Econometrica*, 50(4):987–1007.

Fama, E. F. (1984). Forward and spot exchange rates. *Journal of Monetary Economics*, 14(3):319–338.

Fernández, A., Martínez, P., and Sténeri, L. (2023). Comportamiento de corto y largo plazo del tipo de cambio real en uruguay. *Centro de Investigaciones Económicas – Cinve*. Diciembre de 2023.

Gamboa-Estrada, F. (2016). Carry trade y depreciaciones bruscas del tipo de cambio en colombia. *Borradores de Economia*, 957.

Hassan, T. A. and Mano, R. C. (2014). Forward and spot exchange rates in a multi-currency world. NBER Working Paper 20294, National Bureau of Economic Research, Cambridge, MA.

Hsieh, D. A. (1989). Modeling heteroscedasticity in daily foreign-exchange rates. *Journal of Business & Economic Statistics*, 7(3):307–317.

Inoue, A., Jordà, , and Kuersteiner, G. M. (2023). Significance bands for local projections. Working Paper 2023-15, Federal Reserve Bank of San Francisco.

Jordà, (2005). Estimation and inference of impulse responses by local projections. *American Economic Review*, 95(1):161–182.

Lustig, H., Roussanov, N., and Verdelhan, A. (2008). Common risk factors in currency markets. NBER Working Paper 14082, National Bureau of Economic Research, Cambridge, MA.

Lustig, H. and Verdelhan, A. (2007). The cross-section of foreign currency risk premia and consumption growth risk. *American Economic Review*, 97(1):89–117.

Plagborg-Møller, M. and Wolf, C. K. (2021). Local projections and vars estimate the same impulse responses. *Econometrica*, 89(2):955–980.

Ramey, V. A. (2016). Macroeconomic shocks and their propagation. *Handbook of Macroeconomics*, 2:71–162.

A Appendix

A.1 Appendix A

A.1.1 Additional Tables

Table A.1: Unit Root Tests - Augmented Dickey-Fuller

	ADF t-Stat	p-Value
Level log(USD/UYU)	-1.468	0.834
Diff log(USD/UYU)	-6.609	0.000
Level Rate Diff	-1.047	0.933
Diff Rate Diff	-9.101	0.000

Table A.2: ARCH-LM Test for Autoregressive Conditional Heteroskedasticity

Lags(p)	χ^2	df	Prob $> \chi^2$
1	24.418	1	0.0000
2	24.502	2	0.0000
3	34.340	3	0.0000
4	41.405	4	0.0000
5	46.164	5	0.0000
6	47.770	6	0.0000
7	51.498	7	0.0000
8	51.112	8	0.0000

Note: H_0: No ARCH effects; H_1: ARCH(p) disturbance.

Table A.3: Ljung-Box Test for White Noise

Residuals	Lags	Q-Stat	p-Value
Standardized	4	1.462	0.8334
Standardized	8	13.943	0.0833
Squared Standardized	4	3.257	0.5158
Squared Standardized	8	5.488	0.7044

Note: H_0: No autocorrelation; H_1: Autocorrelation present.

Table A.4: Unit Root Tests - Augmented Dickey-Fuller

	Horizon	Coef_Diff	SE_Diff	Coef_Cum	SE_Cum	Pval_Diff	Pval_Cum
r1	0	0.004	0.008	0.004	0.008	0.663	0.663
r2	1	-0.014	0.008	-0.011	0.012	0.355	0.355
r3	2	0.036	0.011	0.026	0.014	0.071	0.071
r4	3	0.015	0.012	0.041	0.019	0.035	0.035
r5	4	-0.009	0.010	0.031	0.019	0.096	0.096

Table A.5: Local Projections - Response of LRM Demand (1-60 days) to CTR_4 100 Points Increase

	Horizon (weeks)				
Variable	0	1	2	3	4
Δ CTR$_t$	0.00362	-0.01440*	0.03606***	0.01533	-0.00920
	(0.00827)	(0.00809)	(0.01060)	(0.01172)	(0.00960)
Δ CTR$_{t-1}$	-0.01708*	0.03452***	0.01848*	-0.00311	-0.00345
	(0.00898)	(0.00956)	(0.01006)	(0.00883)	(0.01241)
Δ CTR$_{t-2}$	0.03053***	0.01393	0.00126	-0.00925	-0.02918**
	(0.01014)	(0.01130)	(0.01063)	(0.01433)	(0.01336)
LRM Demand$_{t-1}$	-9.8920	-8.7507	-11.4971	-49.3423***	7.2752
	(12.3108)	(6.7371)	(14.1276)	(9.2400)	(10.3848)
LRM Demand$_{t-2}$	-8.6517	-9.6087	-6.6734	40.8604***	-9.7886
	(12.5778)	(7.0440)	(14.1436)	(10.4103)	(8.0345)
Constant	292.47***	289.59***	286.57***	134.20	39.91
	(96.97)	(102.86)	(98.34)	(96.90)	(92.55)
Observations	103	102	101	100	99
F-statistic	11.11	8.83	8.74	6.25	1.98
F p-value	0.0000	0.0000	0.0000	0.0000	0.0882

Note: Newey-West standard errors in parentheses (4 lags). Coefficients multiplied by 100.
$^{*}p < 0.10$, $^{**}p < 0.05$, $^{***}p < 0.01$.
Dependent variable: Moving average-4-period smoothed weekly change in log LRM demand (1-60 days) at horizon h.

Table A.6: Local Projections - Response of LRM Demand (60-120 days) to CTR_13 100 Points Increase

	Horizon (weeks)				
Variable	0	1	2	3	4
Δ CTR$_t$	-0.02572	0.02201	0.04302	0.05783	0.08639
	(0.02307)	(0.04344)	(0.04966)	(0.05516)	(0.06179)
Δ CTR$_{t-1}$	0.03803	0.04620	0.07377	0.09886	0.03418
	(0.03371)	(0.04519)	(0.05504)	(0.06306)	(0.05094)
Δ CTR$_{t-2}$	-0.00770	0.02597	0.08565	0.04572	0.02783
	(0.03895)	(0.05813)	(0.07711)	(0.06098)	(0.06514)
LRM Demand$_{t-1}$	12.9175	1.0849	-19.2818	-65.6981***	-76.5124***
	(9.6716)	(15.4642)	(17.2144)	(21.6775)	(24.5743)
LRM Demand$_{t-2}$	-25.2358**	-28.8280*	-22.3936	16.9244	27.6349
	(9.7930)	(15.3514)	(16.9292)	(19.8250)	(21.1748)
Constant	191.85***	432.03***	649.27***	760.53***	762.84***
	(63.18)	(132.56)	(190.90)	(232.22)	(246.97)
Observations	103	102	101	100	99
F-statistic	3.57	3.22	2.90	3.37	2.73
F p-value	0.0053	0.0098	0.0177	0.0077	0.0240

Note: Newey-West standard errors in parentheses (4 lags). Coefficients multiplied by 100.
$^{*}p < 0.10$, $^{**}p < 0.05$, $^{***}p < 0.01$.
Dependent variable: Moving average-4-period smoothed weekly change in log LRM demand (1-60 days) at horizon h.

Table A.7: Local Projections - Response of LRM Demand (60-120 days) to CTR_{46} 100 Points Increase

	Horizon (weeks)				
Variable	0	1	2	3	4
Δ CTR_t	-0.03571	-0.00187	-0.06612	-0.20681**	0.11405
	(0.14238)	(0.10554)	(0.14112)	(0.09500)	(0.09559)
Δ CTR_{t-1}	0.05070	-0.07113	-0.19439*	0.00798	0.01197
	(0.09635)	(0.14117)	(0.09858)	(0.08506)	(0.08492)
Δ CTR_{t-2}	-0.04208	-0.22087**	0.00569	-0.10522	0.20913
	(0.13801)	(0.10982)	(0.09863)	(0.09631)	(0.13186)
LRM $Demand_{t-1}$	-88.1743***	-69.0956***	-99.0991***	-77.5137***	-106.0170***
	(8.7378)	(10.1276)	(9.5510)	(10.4292)	(10.3956)
LRM $Demand_{t-2}$	28.9268***	-1.2636	20.6445*	-9.0375	25.9427**
	(9.9635)	(9.4441)	(10.5584)	(10.2444)	(11.5596)
Constant	926.24***	1100.03***	1226.99***	1352.96***	1251.62***
	(178.75)	(213.69)	(219.26)	(227.41)	(260.53)
Observations	105	104	103	102	101
F-statistic	28.00	15.25	23.33	17.57	26.10
F p-value	0.0000	0.0000	0.0000	0.0000	0.0000

Note: Newey-West standard errors in parentheses (4 lags). Coefficients multiplied by 100.
$^{*}p < 0.10$, $^{**}p < 0.05$, $^{***}p < 0.01$.
Dependent variable: Cumulative change in log LRM demand (60-120 days) at horizon h.

Table A.8: Local Projections - Response of LRM Demand (1-60 days) to CTR 100 Points Increase (1 Lag)

	Horizon (weeks)				
Variable	0	1	2	3	4
Δ CTR_t	-0.00256	-0.01718*	0.03616***	0.01520	-0.00319
	(0.00890)	(0.00873)	(0.01021)	(0.01006)	(0.01064)
Δ CTR_{t-1}	-0.02136**	0.03191***	0.01871*	-0.00362	-0.00148
	(0.00967)	(0.00891)	(0.01025)	(0.00998)	(0.01190)
LRM $Demand_{t-1}$	-17.6595***	-16.7155***	-17.1007***	-15.5201**	0.85867
	(5.62445)	(5.76823)	(6.05574)	(6.33293)	(6.38013)
Constant	278.4167***	263.6352***	269.7880***	244.6576**	-13.0595
	(88.87219)	(91.16616)	(95.69790)	(100.06030)	(100.69760)
Observations	104	103	102	101	100
F-statistic	6.19	12.87	12.51	2.36	0.04
F p-value	0.0007	0.0000	0.0000	0.0759	0.9903

Note: Newey-West standard errors in parentheses (4 lags). Coefficients multiplied by 100.
$^{*}p < 0.10$, $^{**}p < 0.05$, $^{***}p < 0.01$.
Dependent variable: Cumulative change in log LRM demand (1-60 days) at horizon h.

Table A.9: Local Projections - Cumulative Response of LRM Demand (60-120 days) to CTR 100 Points Increase (1 Lag)

	Horizon (weeks)				
Variable	0	1	2	3	4
Δ CTR$_t$	-0.02598	0.01257	0.01643	0.04620	0.08123
	(0.02901)	(0.04889)	(0.04302)	(0.04744)	(0.05515)
Δ CTR$_{t-1}$	0.02848	0.03099	0.04925	0.09735	0.04075
	(0.03532)	(0.03880)	(0.04907)	(0.05910)	(0.04656)
LRM Demand$_{t-1}$	-10.4490**	-24.7900***	-37.2286***	-49.0170***	-50.9101***
	(4.13003)	(7.75108)	(10.55285)	(13.37675)	(14.38182)
Constant	163.1176**	386.5174***	580.2609***	763.8991***	793.9075***
	(64.27458)	(120.73640)	(164.45720)	(208.56170)	(224.41870)
Observations	104	103	102	101	100
F-statistic	4.00	5.21	5.40	5.43	4.58
F p-value	0.0098	0.0022	0.0018	0.0017	0.0048

Note: Newey-West standard errors in parentheses (4 lags). Coefficients multiplied by 100.
$^{*}p < 0.10$, $^{**}p < 0.05$, $^{***}p < 0.01$.
Dependent variable: Cumulative change in log LRM demand (60-120 days) at horizon h.

Table A.10: Local Projections - Cumulative Response of LRM Demand (120+ days) to CTR 100 Points Increase (1 Lag)

	Horizon (weeks)				
Variable	0	1	2	3	4
Δ CTR$_t$	-0.08522	0.04604	-0.09733	-0.18527**	0.01828
	(0.14672)	(0.09148)	(0.14878)	(0.09010)	(0.09222)
Δ CTR$_{t-1}$	0.00333	-0.03464	-0.21952**	0.01856	-0.06817
	(0.10279)	(0.12733)	(0.10498)	(0.09982)	(0.08505)
LRM Demand$_{t-1}$	-83.7854***	-68.7172***	-96.2544***	-78.4572***	-103.2558***
	(10.71694)	(10.06115)	(10.13369)	(10.62507)	(11.33304)
Constant	1310.312***	1074.379***	1505.015***	1227.069***	1614.179***
	(169.66210)	(158.22550)	(161.30710)	(166.82220)	(178.71840)
Observations	106	105	104	103	102
F-statistic	30.80	20.74	30.95	25.23	29.95
F p-value	0.0000	0.0000	0.0000	0.0000	0.0000

Note: Newey-West standard errors in parentheses (4 lags). Coefficients multiplied by 100.
$^{*}p < 0.10$, $^{**}p < 0.05$, $^{***}p < 0.01$.
Dependent variable: Cumulative change in log LRM demand (120+ days) at horizon h.

Table A.11: Local Projections - Cumulative Response of LRM Demand (1-60 days) to CTR 100 Points Increase (3 Lags)

	Horizon (weeks)				
Variable	0	1	2	3	4
Δ CTR$_t$	0.00436	-0.00903	0.02160	0.03789*	0.02882
	(0.00832)	(0.01166)	(0.01539)	(0.01925)	(0.01876)
Δ CTR$_{t-1}$	-0.01344	0.02173*	0.04075**	0.03460*	0.02649
	(0.00834)	(0.01230)	(0.01827)	(0.01964)	(0.02232)
Δ CTR$_{t-2}$	0.03282***	0.04707***	0.04885***	0.03984*	0.01113
	(0.01062)	(0.01494)	(0.01671)	(0.02029)	(0.02112)
Δ CTR$_{t-3}$	0.01856	0.02263*	0.01760	0.00384	-0.01475
	(0.01399)	(0.01237)	(0.01753)	(0.01771)	(0.02109)
LRM Demand$_{t-1}$	-14.8671	-24.6762*	-33.6634***	-81.3131***	-71.4888***
	(13.29798)	(12.71107)	(10.45896)	(12.92747)	(17.53661)
LRM Demand$_{t-2}$	4.86843	1.62570	-37.7594**	12.8148	3.7180
	(13.38705)	(21.83575)	(18.12941)	(17.53472)	(15.49835)
LRM Demand$_{t-3}$	-11.2658	-17.6513	20.2748	4.9943	-0.1862
	(7.73661)	(16.96807)	(21.43985)	(20.87007)	(18.36619)
Constant	335.4105***	641.9535***	807.2750***	1002.367***	1072.597***
	(113.42010)	(208.08140)	(273.20070)	(336.88040)	(368.60350)
Observations	102	101	100	99	98
F-statistic	8.88	7.19	6.44	9.46	4.78
F p-value	0.0000	0.0000	0.0000	0.0000	0.0001

Note: Newey-West standard errors in parentheses (4 lags). Coefficients multiplied by 100.
$^{*}p < 0.10$, $^{**}p < 0.05$, $^{***}p < 0.01$.
Dependent variable: Cumulative change in log LRM demand (1-60 days) at horizon h.

Table A.12: Local Projections - Cumulative Response of LRM Demand (60-120 days) to CTR 100 Points Increase (3 Lags)

	Horizon (weeks)				
Variable	0	1	2	3	4
Δ CTR$_t$	-0.02625	0.01982	0.03884	0.05449	0.08384
	(0.02312)	(0.04555)	(0.04691)	(0.05085)	(0.05864)
Δ CTR$_{t-1}$	0.04717	0.07240	0.08796	0.10631	0.04550
	(0.03821)	(0.05476)	(0.05878)	(0.06497)	(0.06218)
Δ CTR$_{t-2}$	-0.00373	0.03928	0.07367	0.03078	0.02575
	(0.03918)	(0.05879)	(0.07370)	(0.06199)	(0.07362)
Δ CTR$_{t-3}$	0.03525	0.09305*	0.05504	0.03185	0.03539
	(0.03250)	(0.05261)	(0.04545)	(0.06624)	(0.07778)
LRM Demand$_{t-1}$	13.1863	2.8901	-7.3428	-54.6287**	-70.3994***
	(9.79419)	(16.47625)	(18.46723)	(22.59699)	(23.67189)
LRM Demand$_{t-2}$	-26.6044**	-36.9621	-72.3570***	-29.5269	2.5652
	(12.42608)	(22.43247)	(21.68967)	(25.43170)	(24.04629)
LRM Demand$_{t-3}$	0.5758	4.2916	41.7761**	39.7612*	20.1663
	(7.14484)	(13.45028)	(15.06337)	(18.42131)	(22.23040)
Constant	200.0366***	463.9615***	591.6834***	693.1008***	744.5360***
	(72.84151)	(153.16070)	(199.32780)	(245.92670)	(266.65290)
Observations	102	101	100	99	98
F-statistic	2.18	1.99	3.05	2.59	2.08
F p-value	0.0430	0.0647	0.0063	0.0176	0.0539

Note: Newey-West standard errors in parentheses (4 lags). Coefficients multiplied by 100.
$^{*}p < 0.10$, $^{**}p < 0.05$, $^{***}p < 0.01$.
Dependent variable: Cumulative change in log LRM demand (60-120 days) at horizon h.

Table A.13: Local Projections - Cumulative Response of LRM Demand (120+ days) to CTR 100 Points Increase (3 Lags)

	Horizon (weeks)				
Variable	0	1	2	3	4
Δ CTR$_t$	-0.03940	0.03031	-0.09808	-0.18002*	0.14006
	(0.13089)	(0.10926)	(0.14612)	(0.09076)	(0.09574)
Δ CTR$_{t-1}$	-0.00414	-0.05144	-0.22253**	0.09121	0.04973
	(0.10788)	(0.13699)	(0.10649)	(0.09421)	(0.09612)
Δ CTR$_{t-2}$	-0.08620	-0.20288*	-0.01362	-0.03110	0.24000*
	(0.14876)	(0.10678)	(0.08700)	(0.09766)	(0.13654)
Δ CTR$_{t-3}$	-0.21569**	0.01709	-0.10440	0.21806*	0.08508
	(0.10318)	(0.10447)	(0.09789)	(0.12373)	(0.12511)
LRM Demand$_{t-1}$	-87.0834***	-71.8442***	-97.8474***	-82.5840***	-108.8180***
	(9.51764)	(9.69358)	(9.58584)	(10.35507)	(10.98509)
LRM Demand$_{t-2}$	28.9607***	-2.2129	21.2917**	-9.6588	25.2069**
	(9.91551)	(9.48874)	(10.21406)	(10.23800)	(11.81771)
LRM Demand$_{t-3}$	-5.5760	12.7662	-10.9245	18.4392	12.2292
	(9.75420)	(9.22257)	(10.22136)	(10.75333)	(9.19839)
Constant	995.8490***	958.6197***	1367.414***	1153.557***	1115.977***
	(202.90050)	(251.05840)	(255.93330)	(269.74730)	(290.81440)
Observations	104	103	102	101	100
F-statistic	18.79	19.10	17.12	16.88	19.36
F p-value	0.0000	0.0000	0.0000	0.0000	0.0000

Note: Newey-West standard errors in parentheses (4 lags). Coefficients multiplied by 100.
$^{*}p < 0.10$, $^{**}p < 0.05$, $^{***}p < 0.01$.
Dependent variable: Cumulative change in log LRM demand (120+ days) at horizon h.

A.1.2 Additional Figures

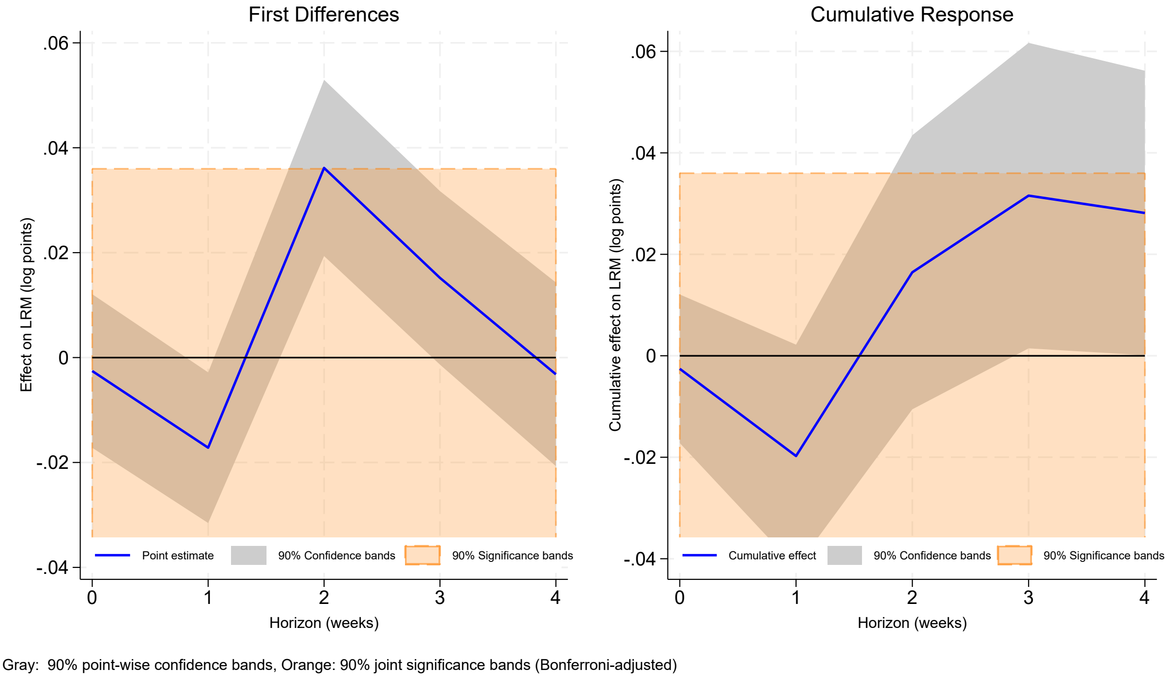

Figure 9: Response of LRM (1–60 days) to a 100-point increase in CTR_4 (1 lag).

Source: own elaboration.

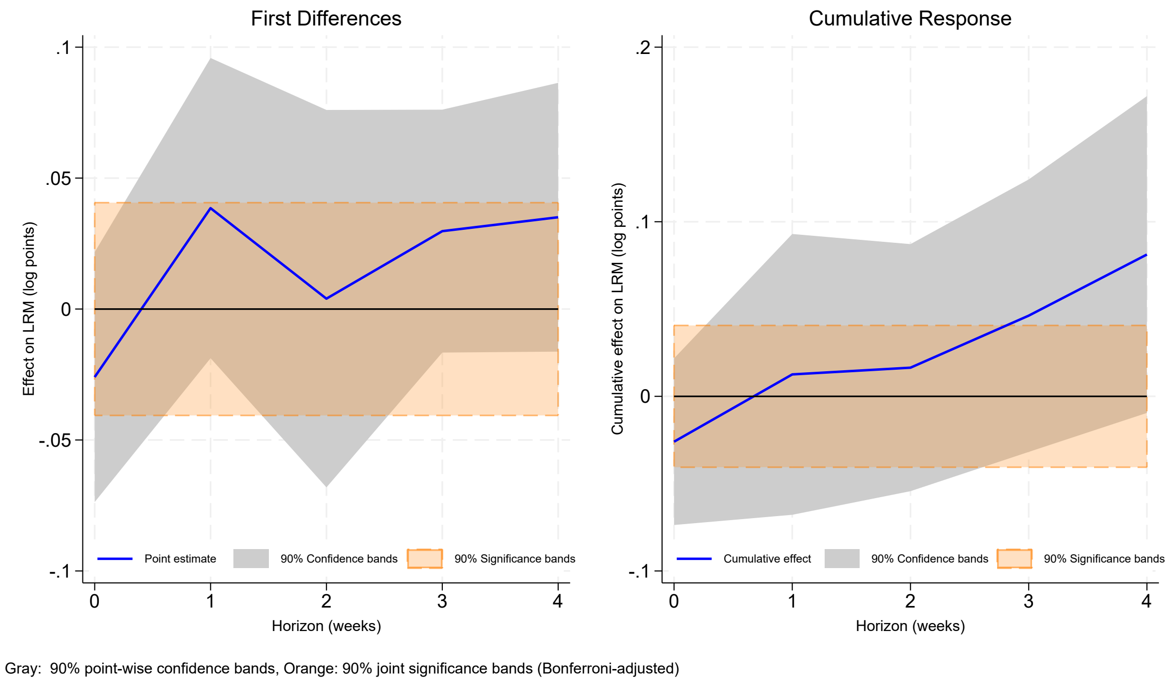

Figure 10: Response of LRM (60-120 days) to a 100-point increase in CTR_{13} (1 lag).

Source: own elaboration.

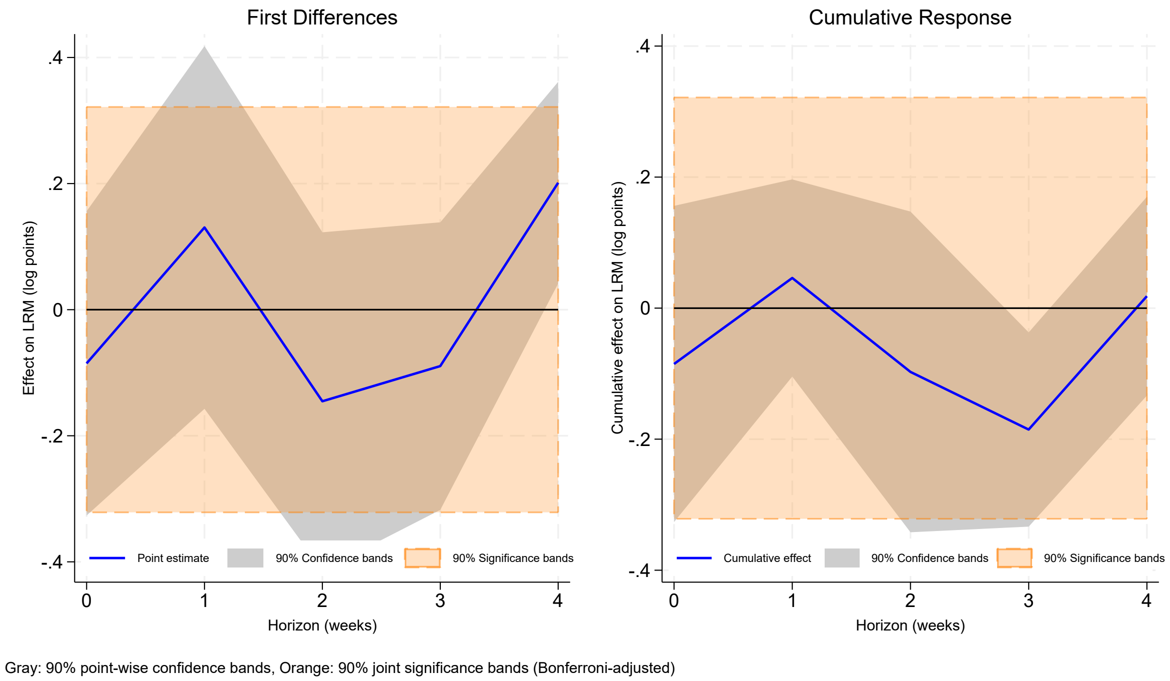

Figure 11: Response of LRM (120+ days) to a 100-point increase in CTR_{46} (1 lag).

Source: own elaboration.

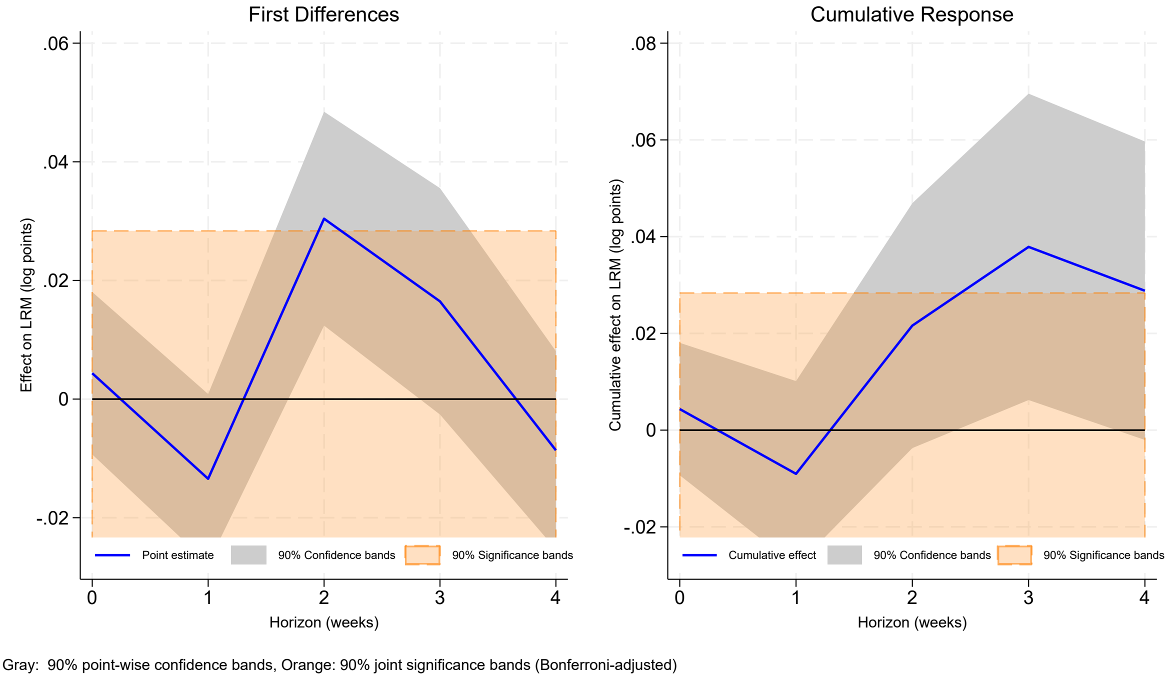

Figure 12: Response of LRM (1–60 days) to a 100-point increase in CTR_4 (3 lags).

Source: own elaboration.

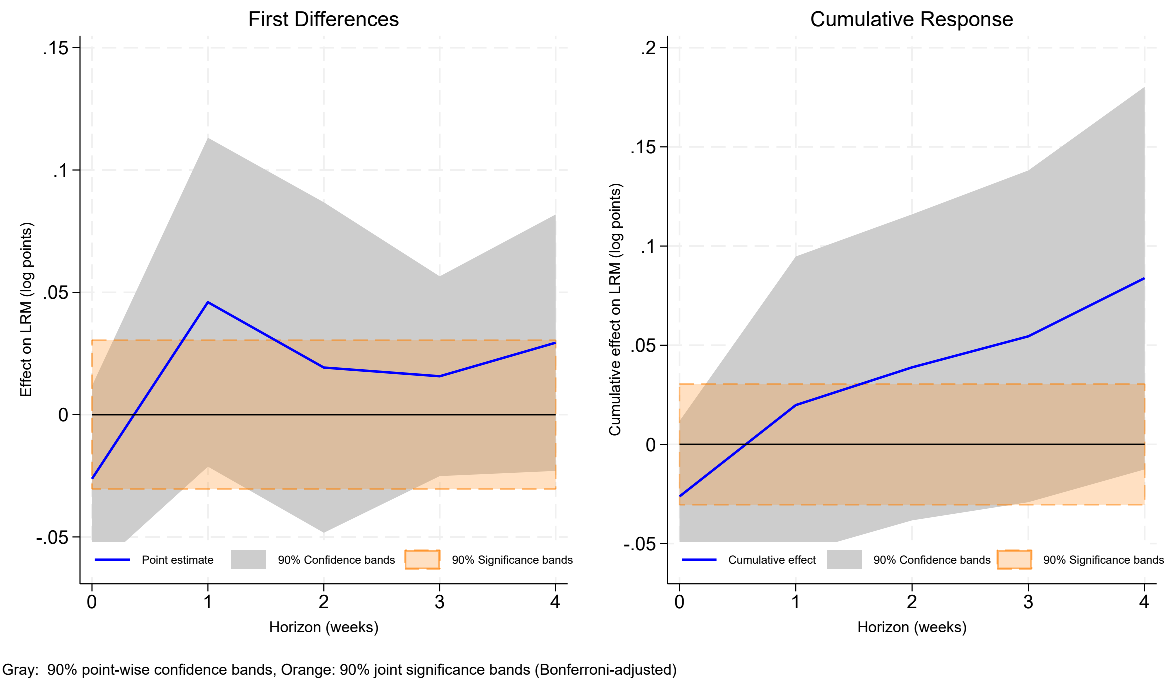

Figure 13: Response of LRM (60-120 days) to a 100-point increase in CTR_{13} (3 lags). *Source: Own elaboration.*

Source: own elaboration.

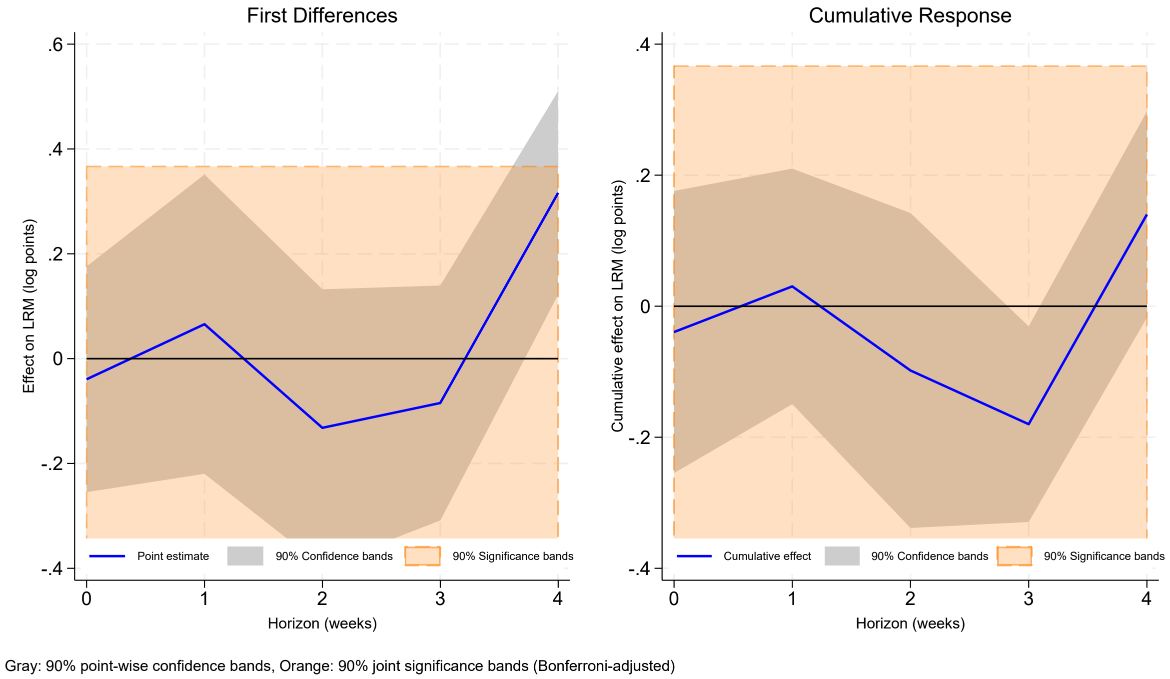

Figure 14: Response of LRM (120+ days) to a 100-point increase in CTR_{46} (3 lags). *Source: Own elaboration.*

Source: own elaboration.

A.2 Appendix B

Table B.1: Summary Statistics

Variable	Obs	Mean	Std. dev.	Min	Max
UY Call Rate	239	8.00	2.44	4.00	11.55
US Fed Funds Rate	239	2.86	2.30	0.06	5.33
Interest Rate Differential	239	5.15	1.55	2.92	8.52
Exchange Rate	239	42.39	2.08	38.77	45.85

Table B.2: Summary Statistics - Final Estimation Sample

Variable	Obs	Mean	Std. dev.	Min	Max
Exchange Rate	108	41.21	1.87	38.77	45.75
Interest Rate Differential	108	4.27	1.13	2.92	6.73
UY Call Rate	108	9.32	1.06	8.00	11.49
US Fed Funds Rate	108	5.05	0.37	4.33	5.33
Log Spread	108	3.718	0.045	3.658	3.823
Delta Log Spread	108	0.0006	0.0069	-0.0136	0.0212
Volatility (4w)	108	0.0068	0.0012	0.0052	0.0113
Volatility (13w)	108	0.0074	0.0005	0.0067	0.0095
Volatility (46w)	108	0.0077	0.0005	0.0070	0.0094
CTR	108	648	215	280	1233
CTR 60d	108	579	145	366	924
CTR 120d	108	553	114	401	775
Demand LRMs (UYU)	108	7,294,582	2,175,188	2,236,430	12,900,000
Demand LRMs 60d (UYU)	108	6,053,410	2,560,952	987,210	12,600,000
Demand LRMs 120d (UYU)	108	6,674,182	2,746,967	2,254,210	20,800,000